A Hybrid SS-ToA Wireless NLoS Geolocation Based on Path Attenuation: ToA Estimation and CRB for Mobile Position Estimation

Bamrung Tau Sieskul, Feng Zheng, and Thomas Kaiser

IEEE Transactions on Vehicular Technology, vol. 58, no. 9, pp. 4930-4942, Nov. 2009.

A Hybrid SS–ToA Wireless NLoS Geolocation Based on Path Attenuation: ToA Estimation and CRB for Mobile Position Estimation

Bamrung Tau Sieskul, *Student Member, IEEE*, Feng Zheng, *Senior Member, IEEE*, and Thomas Kaiser, *Senior Member, IEEE*

***Abstract*—We propose a new hybrid wireless geolocation scheme that requires only one observation quantity, namely, the received signal. The attenuation model is explored herein to capture the propagation features from the received signal. Thus, it provides a more accurate approach for wireless geolocation. To investigate geolocation accuracy, we consider the time-of-arrival (ToA) estimation in the presence of path attenuation. The maximum-correlation (MC) estimator is revisited, and the exact maximum-likelihood (ML) estimator is derived to estimate the ToA. The error performance of the ToA estimates is derived using a Taylor expansion. It is shown that the ML estimate is unbiased and has a smaller error variance than the MC estimate. Numerical results illustrate that, for a low effective bandwidth, the ML estimator well outperforms the MC estimator. Afterward, we derive the Cramér–Rao bound (CRB) for the mobile position estimation. The obtained result, which is applicable to any value of path loss exponents, gives a generalized form of the CRB for the ordinary geolocation approach. In seven hexagonal cells, numerical examples show that the accuracy of the mobile position estimation exploring the path loss is improved compared with that obtained by the usual geolocation.**

***Index Terms*—Non-line-of-sight (NLoS) propagation, parameter estimation, path loss.**

I. Introduction

APPLICATIONS of subscriber location continue to expand in wireless services, e.g., global positioning system, intelligent transport systems, road-side assistance, location-sensitive billing, and mobile yellow pages (see, e.g., [1] and [2], and for indoor, see [3] and [4]). In addition to data communication for wireless networks, user geolocation has been deemed viable due to the emergency requirement by the Federal Communications Commission and the European Commission [5]. In general, two methods can be adopted to find the user position: network-based and handset-based approaches. In the handset-based approach, wireless geolocation is an operation that measures the radio signals traveling between a mobile station (MS) and a set of fixed stations (FSs). The information for radiolocation can be gathered using the signal strength (SS), the angle of arrival, the time of arrival (ToA), the time difference of arrival (TDoA), or their combinations (see, e.g., [6]–[8] and references therein). This information is used to form a location estimate. Toward this end, position location may be conducted in a unilateral or multilateral manner [9]. In the unilateral approach, the MS estimates its own position based on the signal received from the transmitters whose locations are known. For a multilateral system, the MS position is estimated from the signal transmitted by the MS and received at multiple FSs. One of the most important problems in realistic situations is that the system is subject to the sources of errors [10], including multipath propagation [11], non-line-of-sight (NLoS) propagation [12]–[14], and multiple-access interference.

It is well known that the variance of the estimates from any unbiased estimator is bounded by the Cramér–Rao bound (CRB) [15]–[17]. The CRB cannot be attained in general by using finite data but is achievable under regularity conditions by a statistically efficient estimator, e.g., the maximum-likelihood (ML) estimator [18]. For quantifying the inherent accuracy limitation of parameter estimation, the CRB is quite accurate and simple to derive. Recently, the CRB has been analyzed in [19] for several geolocation schemes in the presence of NLoS propagation. It reveals that the Fisher information matrix (FIM) of a hybrid SS–TDoA scheme can be acquired by the superposition of the FIMs from both methods. Hybrid approaches outperform those using only one feature in the aspects of estimation accuracy [20], [21] and reliability [22]. It is worth noting that the frameworks in [19] and [20] are composed of two separate techniques, which require two different measurements: the baseband received signal and the mean SS. Even though both features are jointly formulated via the positioning distance, the parameter estimation needs to collect two kinds of the observation data and then separately be performed. Unfortunately, this combination makes parameter estimation cumbersome.

In this paper, we consider the inherent accuracy of the MS position estimation in a handset-based mutilateral geolocation system using the ToA. Unlike [19] and [20], the SS model and the time delay model are herein combined together to form a composite received-signal model. As a consequence, it requires only the received signal to perform the geolocation.

Manuscript received March 21, 2008; revised May 11, 2009. First published June 2, 2009; current version published November 11, 2009. The review of this paper was coordinated by Prof. Y. Ma.

The authors are with the Institute of Communication Technology, Faculty of Electrical Engineering and Computer Science, Leibniz University Hannover, 30167 Hannover, Germany (e-mail: bamrung.tausieskul@ikt.uni-hannover.de; feng.zheng@ikt.uni-hannover.de; thomas.kaiser@ikt.uni-hannover.de).

Color versions of one or more of the figures in this paper are available online at http://ieeexplore.ieee.org.

Digital Object Identifier 10.1109/TVT.2009.2024156

The novelty, merits, and contributions of this paper can be summarized as follows.

- The novelty of this paper is the ML estimator for the ToA estimation taking into account the information of the path attenuation.
- The merit of this paper is that the following results are shown: The incorporation of the path loss information into the new mobile position estimation algorithm causes no significant additional computation burden but provides better estimation accuracy and a larger positioning range.
- The contributions of this paper lie in the asymptotic error performance analysis. To investigate the accuracy of the mobile position estimation, the corresponding CRB is provided. This result gives a generalized form of the CRB with respect to the usual time delay case.

Some mathematical notations are invoked as follows. $\log_{10}(\cdot)$ is the logarithm of base 10. $(\cdot)^{\mathrm{T}}$ is the transpose of a matrix. $\doteq$ denotes the equivalence from neglecting an irrelevant term. The little "o" in $u(\tau-\tau_b)=o(v(\tau-\tau_b))$ stands for $\lim_{\tau\to\tau_b}(u(\tau-\tau_b)/v(\tau-\tau_b))=0$. $\Re(\cdot)$ is the real part. $(\cdot)^*$ denotes the complex conjugate. $\mathrm{E}_{\mathbf{n}(t)}\{\cdot\}$ is the expectation with respect to $\mathbf{n}(t)$. $(\cdot)^{-1}$ is the inverse operator. $\mathbf{B}\succeq\mathbf{C}$ means that the difference matrix $\mathbf{D}=\mathbf{B}-\mathbf{C}$ is positive semidefinite. $\mathrm{tr}(\cdot)$ is the trace operator. $[\mathbf{M}]_{[2\times 2]}$ is the first 2×2 block of $\mathbf{M}$. $\delta_{\cdot,\cdot}$ is the Kronecker delta function, which is equal to one when its arguments are equal and zero otherwise.

The rest of this paper is organized as follows. In Section II, the path loss model is presented for the wireless geolocation in the presence of NLoS. In Section III, we analyze the error of the time delay estimate. In Section IV, the CRB is derived for the proposed geolocation model. In Section V, numerical examples are presented for various scenarios. Finally, the conclusion is drawn in Section VI.

II. System Model

Let us consider an MS transmitting a radio signal through a wireless channel to a number of base stations (BSs). Let B be the number of all BSs, whose locations, i.e., $\mathbf{p}_b=[x_b \quad y_b]^{\mathrm{T}}$, $b\in\{1,2,\ldots,B\}$, are known. We assume that there is no additional loss of energy, except the path loss attenuation, for the transmitted signal when radio waves propagate in media. There is, however, attenuation in the channel. At each BS, the received energy at the bth BS can be expressed by (see, e.g., [23, p. 46] and [24, p. 38])

$$E_b=\frac{d_0^{\gamma_b}}{d_b^{\gamma_b}}\kappa E_{\mathrm{s}} \tag{1}$$

where d_0 is the close-in reference in the far-field region, d_b is the distance between the MS and the bth BS, γ_b is the path loss exponent at the bth BS, $E_{\mathrm{s}}=\int_{-\infty}^{\infty}|s(t)|^2dt$ is the energy of transmitted signal $s(t)$, and κ is the unitless constant depending on the antenna characteristics and average channel attenuation, which is given by

$$\kappa=\frac{c^2}{16\pi^2 f_0^2 d_0^2} \tag{2}$$

with f_0 being the center frequency of the wireless system and c being the speed of light. At $f_0=1.9$ GHz and for $d_0=100$ m, it is shown in [25] that $\kappa_{\mathrm{dB}}=10\log_{10}(\kappa)\approx -78$ dB. Let $M<B-1$ be the number of the BSs that receive a set $\mathcal{N}\in\{1,2,\ldots,M\}$ of NLoS signals. The line-of-sight (LoS)/NLoS detection for the considered problem is beyond the scope of this paper and can be left for future work. Readers are referred to [26] and [27] for various ideas of identifying the LoS and NLoS. The channel is assumed herein to be static such that 1) the large-scale fading is considered as a spatial average over the small-scale fluctuations of the signals [28, p. 847] and 2) the excess propagation distances $\{l_m\}_{m=1}^{M}$ are constant over the observation period.[1] Let τ_b be the time delay of received signal at the bth BS

$$\tau_b(x,y,l_b)=\frac{1}{c}\left(\sqrt{\tilde{x}_b^2+\tilde{y}_b^2}+l_b\right) \tag{3}$$

where $\tilde{x}_b=x-x_b$ and $\tilde{y}_b=y-y_b$ are the relative distances, $l_b=0$ means no additional propagation distance for the LoS $b\in\{M+1,M+2,\ldots,B\}$, and $l_m>0$ is the additional propagation distance for the NLoS $m\in\{1,2,\ldots,M\}$. As $d_b=c\tau_b$, the energy based on (1) can be rewritten as

$$E_b=\frac{1}{\left(\sqrt{\left(\frac{\tilde{x}_b}{d_0}\right)^2+\left(\frac{\tilde{y}_b}{d_0}\right)^2}+\frac{l_b}{d_0}\right)^{\gamma_b}}\kappa E_{\mathrm{s}}. \tag{4}$$

Since (1) and (4) are valid only in the far field, it is assumed that d_0 is less than $\sqrt{\tilde{x}_b^2+\tilde{y}_b^2}$. This means that, within a circle of radius d_0, there are no BSs. Note that, for free-space path loss, the path loss exponent is $\gamma_b=2$ [29, p. 304], [30, p. 88], while for a wireless environment, the path loss exponent can be less than two [23, p. 47]. The range of the path loss exponent is wide due to the attenuation caused by scattering objects. The received baseband signal can be written as [19]

$$r_b(t)=a_b s(t-\tau_b)+n_b(t) \tag{5}$$

where $s(t)$ is the known waveform, a_b and τ_b are the amplitude and the time delay of the propagation to the bth BS, and $n_b(t)$ is an additive noise at the bth BS that is assumed to be a complex-valued zero-mean white Gaussian process with double-sided power spectral density N_0 (in joules) [31, eq. (8.17)]. Assume that the transmitted signal is nonzero only in the interval $(0,T_{\mathrm{s}}]$, where T_{s} is the signal period. The relation among the received energy, the transmitted energy, and the path gain can be postulated as $E_b=a_b^2E_{\mathrm{s}}$. The amplitude can then be shown as

$$a_b=\frac{1}{\left(\sqrt{\left(\frac{\tilde{x}_b}{d_0}\right)^2+\left(\frac{\tilde{y}_b}{d_0}\right)^2}+\frac{l_b}{d_0}\right)^{\frac{1}{2}\gamma_b}}\sqrt{\kappa}. \tag{6}$$

In this model, we can see that $r_b(t)$ is a random signal caused by the randomness of $n_b(t)$. Since the position $\mathbf{p}$ and the

[1] For random NLoS excess propagation paths, if the knowledge of the distribution of l_m is available, the parameter estimation can be cast into a *maximum a posteriori* approach [19].

nuisance parameter l_b are unknown and deterministic, so are their reparameterizations a_b and τ_b. All the unknown parameters can be aggregated into the vector $\boldsymbol{\theta} \in \mathbb{R}^{(M+2)\times 1}$ as

$$\boldsymbol{\theta} = [\mathbf{p}^{\mathrm{T}} \quad \mathbf{l}^{\mathrm{T}}]^{\mathrm{T}} \tag{7}$$

where $\mathbf{l} \in \mathbb{R}^{M\times 1}$ is given by

$$\mathbf{l} = [\, l_1 \quad l_2 \quad \cdots \quad l_M \,]^{\mathrm{T}}. \tag{8}$$

The problem of the parameter estimation can be stated as follows. Given the observation $\{r_b(t)\}_{b=1}^{B}$ over the period $t \in (0, T]$ for $T > 0$ in which $\boldsymbol{\theta}$ is invariant, find the unknown parameter $\boldsymbol{\theta}$. The solution to this problem can uniquely be determined [32] when the number of the received signals B is equal to or larger than the number of the unknown parameters $M + 2$. It means that $B \geq M + 2$. This condition is assumed to be held throughout this paper, since the FIM will be of full rank, and thus, the performance bound of the mobile position estimate can be evaluated.

Assume that the discrimination between the LoS and NLoS propagations has been conducted. The received-signal amplitudes $\{a_b\}_{b=1}^{B}$ and the positive delay distances $\{l_m\}_{m=1}^{M}$ are assumed to be unknown, whereas the position of the MS, i.e., $\mathbf{p} = [x \quad y]^{\mathrm{T}}$, is the parameter of interest.

Let the solution of the homogeneous Fredholm integral equation

$$\lambda_{b,k} f_{b,k}(t) = \int_0^T \varphi_b(t, \acute{t}) f_{b,k}(\acute{t}) d\acute{t}, \qquad k \in \{1, 2 \ldots, K\} \tag{9}$$

be the eigenvalue $\lambda_{b,k}$ and the orthonormal function $f_{b,k}(t)$, where the kernel $\varphi_b(t, \acute{t})$ is the eigenfunction of the noise autocovariance function. According to the Karhunen–Loève expansion (see, e.g., [33, p. 37], [34, p. 279], and [35, p. 298]), the signal can be represented as

$$r_b(t) = \lim_{K\to\infty} \sum_{k=1}^{K} r_{b,k} f_{b,k}(t) \tag{10}$$

where the received-signal sample is given by $r_{b,k} = \int_0^T f_{b,k}(t) r_b(t) dt$. From (5), the received-signal sample can be expressed as

$$r_{b,k} = a_b s_{b,k} + n_{b,k} \tag{11}$$

where the signal and noise samples are given by $s_{b,k} = \int_0^T f_{b,k}(t) s(t - \tau_b) dt$ and $n_{b,k} = \int_0^T f_{b,k}(t) n_b(t) dt$. Assume that the basis function $f_{b,k}(t)$ is chosen such that the noise samples $\{n_{b,k}\}_{k=1}^{K}$ are identically and independently distributed. The probability density function (pdf) of the complex Gaussian random multivariate $\{r_{b,k}\}_{k=1}^{K}$ can be written as

$$p(r_{b,1}, \ldots, r_{b,K}|\tau_b) = \frac{1}{(\pi N_0)^K} e^{-\frac{1}{N_0}\sum_{k=1}^{K} |r_{b,k} - a_b s_{b,k}|^2}. \tag{12}$$

Given the continuous signal $r_b(t); t \in (0, T]$, the likelihood of τ_b can be written in the logarithmic scale as

$$\begin{aligned}\ell\left(\tau_b|r_b(t); t \in (0, T]\right) &= \lim_{K\to\infty} \ln\left(p(r_{b,1}, \ldots, r_{b,K}|\tau_b)\right) \\ &\doteq -\frac{1}{N_0} \int_0^T |r_b(t) - a_b s(t - \tau_b)|^2 \, dt.\end{aligned} \tag{13}$$

Assume that the noises from different BSs are independent of each other. Given the received signal from all BSs

$$\mathbf{r}(t) = [\, r_1(t) \quad r_2(t) \quad \cdots \quad r_B(t) \,]^{\mathrm{T}} \tag{14}$$

the log likelihood of $\boldsymbol{\tau}$ is given by

$$\ell\left(\boldsymbol{\tau}|\mathbf{r}(t); t \in (0, T]\right) \doteq -\frac{1}{N_0} \sum_{b=1}^{B} \int_0^T |r_b(t) - a_b s(t - \tau_b)|^2 \, dt. \tag{15}$$

III. ToA Estimation and Performance Analysis

Let us determine the first and second derivatives of a_b from

$$\frac{\partial}{\partial \tau} a_b(\tau) = -\frac{1}{2}\frac{1}{\tau}\gamma_b a_b(\tau) \tag{16a}$$

$$\frac{\partial^2}{\partial \tau^2} a_b(\tau) = \frac{1}{2}\frac{1}{\tau^2}\left(1 + \frac{1}{2}\gamma_b\right)\gamma_b a_b(\tau). \tag{16b}$$

Let $\rho_{\mathrm{ss},b}(\tau)$ be the correlation function between the transmitted signal with the true time delay and the transmitted signal with a delayed time τ defined by

$$\rho_{\mathrm{ss},b}(\tau) = \int_0^T \Re\left(s^*(t - \tau_b) s(t - \tau)\right) dt. \tag{17}$$

Assume that the transmitted signal is continuously differentiable up to the second order. Taking the second-order Taylor series of $\rho_{\mathrm{ss},b}(\tau)$ around the true value of the time delay, i.e., τ_b, we can see that [36, App. 2.1]

$$\begin{aligned}\rho_{\mathrm{ss},b}(\tau) &= \rho_{\mathrm{ss},b}(\tau_b) + \left.\frac{\partial}{\partial \tau}\rho_{\mathrm{ss},b}(\tau)\right|_{\tau=\tau_b} (\tau - \tau_b) \\ &\quad + \frac{1}{2!}\left.\frac{\partial^2}{\partial \tau^2}\rho_{\mathrm{ss},b}(\tau)\right|_{\tau=\tau_b} (\tau - \tau_b)^2 + o\left((\tau - \tau_b)^3\right).\end{aligned} \tag{18}$$

Let us consider

$$\begin{aligned}&\left.\frac{\partial}{\partial \tau}\rho_{\mathrm{ss},b}(\tau)\right|_{\tau=\tau_b} \\ &= -\left.\int_{-\tau}^{T-\tau} \Re\left(s\left(t' - (\tau_b - \tau)\right)\frac{\partial}{\partial t'} s^*(t')\right) dt'\right|_{\tau=\tau_b} \\ &= -\frac{1}{2}\left.|s(t)|^2\right|_{t=-\tau_b}^{T-\tau_b} \\ &= 0\end{aligned} \tag{19a}$$

$$\begin{aligned}\frac{\partial^2}{\partial\tau^2}\rho_{\mathrm{ss},b}(\tau)\bigg|_{\tau=\tau_b} &= \int_{-\tau}^{T-\tau}\Re\left(s\left(t'-(\tau_b-\tau)\right)\frac{\partial^2}{\partial t'^2}s^*(t')\right)dt'\bigg|_{\tau=\tau_b}\\ &= \Re\left(s(t)\frac{\partial}{\partial t}s^*(t)\right)\bigg|_{t=-\tau_b}^{T-\tau_b} - \int_{-\tau_b}^{T-\tau_b}\left|\frac{\partial}{\partial t}s(t)\right|^2 dt\\ &= -\int_{-\infty}^{\infty}\left|\frac{\partial}{\partial t}s(t)\right|^2 dt\\ &= -4\pi^2 E_{\mathrm{s}}\bar{\beta}^2 \end{aligned} \tag{19b}$$

where $\bar{\beta}$ is the effective (root-mean-square) bandwidth defined by

$$\bar{\beta} = \sqrt{\frac{\int_{-\infty}^{\infty} f^2\,|S(f)|^2\,df}{\int_{-\infty}^{\infty}|S(f)|^2\,df}} \tag{20}$$

with $S(f)$ being the Fourier transform of $s(t)$. Let $\rho_{\mathrm{ns},b}(\tau)$, $\dot{\rho}_{\mathrm{ns},b}(\tau)$, and $\ddot{\rho}_{\mathrm{ns},b}(\tau)$ be the random correlations defined by

$$\rho_{\mathrm{ns},b}(\tau) = \int_0^T \Re\left(n_b^*(t)s(t-\tau)\right)dt \tag{21a}$$

$$\dot{\rho}_{\mathrm{ns},b}(\tau) = \int_0^T \Re\left(n_b^*(t)\frac{\partial}{\partial\tau}s(t-\tau)\right)dt \tag{21b}$$

$$\ddot{\rho}_{\mathrm{ns},b}(\tau) = \int_0^T \Re\left(n_b^*(t)\frac{\partial^2}{\partial\tau^2}s(t-\tau)\right)dt. \tag{21c}$$

It can be shown that

$$\mathrm{E}_{n_b(t)}\left\{\rho_{\mathrm{ns},b}(\tau)\right\} = 0 \tag{22a}$$

$$\mathrm{E}_{n_b(t)}\left\{\dot{\rho}_{\mathrm{ns},b}(\tau)\right\} = 0 \tag{22b}$$

$$\mathrm{E}_{n_b(t)}\left\{\ddot{\rho}_{\mathrm{ns},b}(\tau)\right\} = 0 \tag{22c}$$

$$\mathrm{E}_{n_b(t)}\left\{\rho_{\mathrm{ns},b}(\tau)\dot{\rho}_{\mathrm{ns},b}(\tau)\right\} = 0 \tag{22d}$$

$$\mathrm{E}_{n_b(t)}\left\{\rho_{\mathrm{ns},b}(\tau)\ddot{\rho}_{\mathrm{ns},b}(\tau)\right\} = -2\pi^2 E_{\mathrm{s}}\bar{\beta}^2 N_0 \tag{22e}$$

$$\mathrm{E}_{n_b(t)}\left\{\rho^2_{\mathrm{ns},b}(\tau)\right\} = \frac{1}{2}E_{\mathrm{s}}N_0 \tag{22f}$$

$$\mathrm{E}_{n_b(t)}\left\{\dot{\rho}^2_{\mathrm{ns},b}(\tau)\right\} = 2\pi^2 E_{\mathrm{s}}\bar{\beta}^2 N_0. \tag{22g}$$

Let $f_b(\tau)$ be any objective function, which is differentiable up to the second order. Taking the first-order Taylor series of $(\partial/\partial\tau)f_b(\tau)$ around the true value τ_b, we arrive at (see, e.g., [37, eq. (17 - 9.2)] and [33, eq. (6 - 50)])

$$\frac{\partial}{\partial\tau}f_b(\tau) = \frac{\partial}{\partial\tau}f_b(\tau)\bigg|_{\tau=\tau_b} + (\tau-\tau_b)\,\frac{\partial^2}{\partial\tau^2}f_b(\tau)\bigg|_{\tau=\tau_b} + o\left((\tau-\tau_b)^2\right). \tag{23}$$

At the estimated point $\tau=\hat{\tau}_b$, we obtain [38, p. 240]

$$0 = \frac{\partial}{\partial\tau}f_b(\tau)\bigg|_{\tau=\tau_b} + (\hat{\tau}_b-\tau_b)\,\frac{\partial^2}{\partial\tau^2}f_b(\tau)\bigg|_{\tau=\breve{\tau}_b} \tag{24}$$

where $\breve{\tau}_b$ lies in the line segment between τ_b and $\hat{\tau}_b$. For a continuous derivative $(\partial^2/\partial\tau^2)f_b(\tau)$, the quantity $(\partial^2/\partial\tau^2) f_b(\tau)|_{\tau=\breve{\tau}_b}$ converges to $\mathrm{E}_{n_b(t)}\{(\partial^2/\partial\tau^2)f_b(\tau)|_{\tau=\tau_b}\}$ with probability one [38, Ch. 8]. As a result, the time delay estimation error in (24) converges to

$$\hat{\tau}_b-\tau_b \cong -\frac{\frac{\partial}{\partial\tau}f_b(\tau)\big|_{\tau=\tau_b}}{\mathrm{E}_{n_b(t)}\left\{\frac{\partial^2}{\partial\tau^2}f_b(\tau)\Big|_{\tau=\tau_b}\right\}}. \tag{25}$$

In the sequel, two kinds of ToA estimators and their performance analysis are presented.

A. MC Estimator

Let $\rho_b(\tau)$ be the correlation function between the received signal and a delayed replica of the transmitted waveform defined by

$$\rho_b(\tau) = \int_0^T \Re\left(r_b^*(t)s(t-\tau)\right)dt. \tag{26}$$

The time delay estimate of the maximum-correlation (MC) estimator is defined as

$$\hat{\tau}_{\mathrm{MC},b} = \arg\max_{\tau}\rho_b(\tau). \tag{27}$$

Substituting (5) into (26) and differentiating $\rho_b(\tau)$ with respect to the unknown parameter τ, we have

$$\frac{\partial}{\partial\tau}\rho_b(\tau) = a_b\left(\frac{\partial}{\partial\tau}\rho_{\mathrm{ss},b}(\tau)\right) + \dot{\rho}_{\mathrm{ns},b}(\tau) \tag{28a}$$

$$\frac{\partial^2}{\partial\tau^2}\rho_b(\tau) = a_b\left(\frac{\partial^2}{\partial\tau^2}\rho_{\mathrm{ss},b}(\tau)\right) + \ddot{\rho}_{\mathrm{ns},b}(\tau). \tag{28b}$$

Note that a_b is the path gain at the true value τ_b. Substituting (19a) and (19b) into (28a) and (28b), respectively, for $\tau_b=\hat{\tau}_b$, we obtain

$$\frac{\partial}{\partial\tau}\rho_b(\tau)\bigg|_{\tau=\tau_b} = \dot{\rho}_{\mathrm{ns},b}(\tau_b) \tag{29a}$$

$$\frac{\partial^2}{\partial\tau^2}\rho_b(\tau)\bigg|_{\tau=\tau_b} = -4\pi^2 E_{\mathrm{s}}\bar{\beta}^2 a_b + \ddot{\rho}_{\mathrm{ns},b}(\tau_b). \tag{29b}$$

Substituting (29a) and (29b) into (25), the time delay estimation error of the MC estimator can be written as

$$\begin{aligned}\hat{\tau}_{\mathrm{MC},b}-\tau_b &\cong -\frac{\frac{\partial}{\partial\tau}\rho_b(\tau)\big|_{\tau=\tau_b}}{\mathrm{E}_{n_b(t)}\left\{\frac{\partial^2}{\partial\tau^2}\rho_b(\tau)\Big|_{\tau=\tau_b}\right\}}\\ &= \frac{\dot{\rho}_{\mathrm{ns},b}(\tau_b)}{4\pi^2 E_{\mathrm{s}}\bar{\beta}^2 a_b}.\end{aligned} \tag{30}$$

From (22a) and (22f), the bias and error variance can be written as

$$\mathrm{E}_{n_b(t)}\{\hat{\tau}_{\mathrm{MC},b}-\tau_b\}=0 \tag{31a}$$

$$\begin{aligned}\mathrm{E}_{n_b(t)}\left\{(\hat{\tau}_{\mathrm{MC},b}-\tau_b)^2\right\}&=\mathrm{E}_{n_b(t)}\left\{\frac{\dot{\rho}^2_{\mathrm{ns},b}(\tau_b)}{(4\pi^2E_\mathrm{s}\bar{\beta}^2a_b)^2}\right\}\\&=\frac{1}{\frac{E_\mathrm{s}}{N_0}8\pi^2\bar{\beta}^2a_b^2}.\end{aligned} \tag{31b}$$

The error performance shown above is similar to a standard benchmark, e.g., CRB, for the time delay estimation based on a distance-independent path gain [33], [37], [39].

B. ML Estimator

From (15), the natural logarithm of the pdf of the received signal can be written as

$$\begin{aligned}\ell\left(\boldsymbol{\tau}|\mathbf{r}(t);t\in(0,T]\right)\doteq-\frac{1}{N_0}E_\mathrm{s}\sum_{b=1}^{B}a_b^2\\-2a_b\int_0^T\Re\left(r_b^*(t)s(t-\tau_b)\right)dt.\end{aligned} \tag{32}$$

The ML estimate of the time delay is therefore given by

$$\begin{aligned}\hat{\boldsymbol{\tau}}_\mathrm{ML}&=\arg\max_{\boldsymbol{\tau}}p\left(\mathbf{r}(t);t(0,T]|\boldsymbol{\theta}\right)\\&=\arg\max_{\boldsymbol{\tau}}\ell\left(\boldsymbol{\tau}|\mathbf{r}(t);t\in(0,T]\right)\\&=\arg\min_{\boldsymbol{\tau}}E_\mathrm{s}\sum_{b=1}^{B}a_b^2(\tau)\\&\quad-2a_b(\tau)\int_0^T\Re\left(r_b^*(t)s(t-\tau)\right)dt\end{aligned} \tag{33}$$

where $\boldsymbol{\tau}\in\mathbb{R}_+^{B\times1}$ lies in the domain of positive values. The ML estimate can separately be solved by

$$\hat{\tau}_{\mathrm{ML},b}=\arg\min_{\tau}\zeta_b(\tau) \tag{34}$$

where $\zeta_b(\tau)$ is the objective function defined by

$$\zeta_b(\tau)=a_b^2(\tau)E_\mathrm{s}-2a_b(\tau)\rho_b(\tau). \tag{35}$$

From (16a) and (16b), the first and second derivatives of the objective function follow:

$$\begin{aligned}\frac{\partial}{\partial\tau}\zeta_b(\tau)=&-\frac{1}{\tau}\gamma_b\left(E_\mathrm{s}a_b(\tau)-\rho_b(\tau)\right)a_b(\tau)\\&-2a_b(\tau)\frac{\partial}{\partial\tau}\rho_b(\tau)\end{aligned} \tag{36}$$

$$\begin{aligned}\frac{\partial^2}{\partial\tau^2}\zeta_b(\tau)=&\frac{1}{\tau^2}\gamma_b(\gamma_b+1)E_\mathrm{s}a_b^2(\tau)-2a_b(\tau)\frac{\partial^2}{\partial\tau^2}\rho_b(\tau)\\&+\frac{1}{\tau}2\gamma_ba_b(\tau)\frac{\partial}{\partial\tau}\rho_b(\tau)\\&-\frac{1}{\tau^2}\rho_b(\tau)\left(1+\frac{1}{2}\gamma_b\right)\gamma_ba_b(\tau).\end{aligned} \tag{37}$$

Substituting $\rho_b(\tau_b)=a_bE_\mathrm{s}+\rho_{\mathrm{ns},b}(\tau_b)$, (29a), and (29b) into (36) and (37), we obtain

$$\left.\frac{\partial}{\partial\tau}\zeta_b(\tau)\right|_{\tau=\tau_b}=\frac{1}{\tau_b}\gamma_ba_b\rho_{\mathrm{ns},b}(\tau_b)-2a_b\dot{\rho}_{\mathrm{ns},b}(\tau_b) \tag{38}$$

$$\begin{aligned}\left.\frac{\partial^2}{\partial\tau^2}\zeta_b(\tau)\right|_{\tau=\tau_b}=&\frac{1}{2}\frac{1}{\tau_b^2}\gamma_b^2E_\mathrm{s}a_b^2+8\pi^2E_\mathrm{s}\bar{\beta}^2a_b^2\\&-2a_b\ddot{\rho}_{\mathrm{ns},b}(\tau_b)+\frac{1}{\tau_b}2\gamma_ba_b\dot{\rho}_{\mathrm{ns},b}(\tau_b)\\&-\frac{1}{\tau_b^2}\left(1+\frac{1}{2}\gamma_b\right)\gamma_ba_b\rho_{\mathrm{ns},b}(\tau_b).\end{aligned} \tag{39}$$

Using $\mathrm{E}_{n_b(t)}\{\rho_{\mathrm{ns},b}(\tau_b)\}=0$, $\mathrm{E}_{n_b(t)}\{\dot{\rho}_{\mathrm{ns},b}(\tau_b)\}=0$, $\mathrm{E}_{n_b(t)}\{\ddot{\rho}_{\mathrm{ns},b}(\tau_b)\}=0$, (38) and (39), the time delay estimation error in (34) converges to

$$\begin{aligned}\hat{\tau}_{\mathrm{ML},b}-\tau_b\cong&-\frac{\left.\frac{\partial}{\partial\tau}\zeta_b(\tau)\right|_{\tau=\tau_b}}{\mathrm{E}_{n_b(t)}\left\{\left.\frac{\partial^2}{\partial\tau^2}\zeta_b(\tau)\right|_{\tau=\tau_b}\right\}}\\=&\frac{\tau_b\left(2\tau_b\dot{\rho}_{\mathrm{ns},b}(\tau_b)-\gamma_b\rho_{\mathrm{ns},b}(\tau_b)\right)}{E_\mathrm{s}\left(\frac{1}{2}\gamma_b^2+8\pi^2\bar{\beta}^2\tau_b^2\right)a_b}.\end{aligned} \tag{40}$$

Taking the expectation of (40) with respect to $n_b(t)$, we have

$$\mathrm{E}_{n_b(t)}\{\hat{\tau}_{\mathrm{ML},b}-\tau_b\}=0. \tag{41}$$

As $\mathrm{E}_{n_b(t)}\{\rho_{\mathrm{ns},b}(\tau_b)\dot{\rho}_{\mathrm{ns},b}(\tau_b)\}=0$ and $\mathrm{E}_{n_b(t)}\{\dot{\rho}^2_{\mathrm{ns},b}(\tau_b)\}=2\pi^2\bar{\beta}^2E_\mathrm{s}N_0$, we have

$$\mathrm{E}_{n_b(t)}\left\{(\hat{\tau}_{\mathrm{ML},b}-\tau_b)^2\right\}=\frac{1}{\frac{E_\mathrm{s}}{N_0}\left(8\pi^2\bar{\beta}^2+\frac{1}{2\tau_b^2}\gamma_b^2\right)a_b^2}. \tag{42}$$

Remark 1: It can be verified that the CRB for the ToA estimation yields the same expression as (42). We can see that $(1/(E_\mathrm{s}/N_0)8\pi^2\bar{\beta}^2a_b^2(1+(1/16\pi^2\bar{\beta}^2\tau_b^2)\gamma_b^2))\leq(1/(E_\mathrm{s}/N_0)8\pi^2\bar{\beta}^2a_b^2)$, i.e., the ML estimation error variance in (42) is less than that of the MC estimation in (31b), where the equality holds for $\gamma_b=0$. In fact, the equality will never hold, since for free space, the path loss exponent is $\gamma_b=2$ (see, e.g., [29, p. 304] and [30, p. 88]), while for wireless environment, the path loss exponent can be less than two but larger than zero (see, e.g., [23, p. 47]). The performance improvement thus exists and is significant when τ_b is small and γ_b is large. If the bandwidth is large, the error variance of the time delay estimated by the ML tends to the same value as that of the MC estimation error variance.

IV. Cramér–Rao Lower Bound

Let $\hat{\boldsymbol{\theta}}$ be any unbiased estimate of $\boldsymbol{\theta}$. Then, the accuracy of $\hat{\boldsymbol{\theta}}$ is bounded by the Cramér–Rao inequality (see, e.g., [15]–[17])

$$\mathrm{E}_{\mathbf{n}(t)}\left\{(\hat{\boldsymbol{\theta}}-\boldsymbol{\theta})(\hat{\boldsymbol{\theta}}-\boldsymbol{\theta})^\mathrm{T}\right\}\succeq\mathbf{J}_{\boldsymbol{\theta}\boldsymbol{\theta}}^{-1} \tag{43}$$

where $\mathbf{J}_{\boldsymbol{\theta}\boldsymbol{\theta}}\in\mathbb{R}^{(M+2)\times(M+2)}$ is the FIM of $p(\mathbf{r}(t);t\in(0,T]|\boldsymbol{\theta})$. Let us define the total positioning accuracy of both axes as

$$\epsilon^2=\mathrm{E}_{\mathbf{n}(t)}\left\{(\hat{x}-x)^2+(\hat{y}-y)^2\right\}\geq\mathrm{tr}\left(\left[\mathbf{J}_{\boldsymbol{\theta}\boldsymbol{\theta}}^{-1}\right]_{[2\times2]}\right). \tag{44}$$

Proposition 1: Given any unbiased estimates of x and y, which is denoted by $\hat{x}$ and $\hat{y}$, respectively, the variance of the estimation error is bounded by

$$\epsilon^2 \geq \frac{2\sum_{b=M+1}^{B}\chi_b}{\frac{E_s}{N_0}\sum_{b_1=M+1}^{B}\sum_{b_2=M+1}^{B}\chi_{b_1}\chi_{b_2}\sin^2(\phi_{b_2}-\phi_{b_1})} \quad (45)$$

where χ_b and ϕ_b are given by

$$\chi_b = \frac{1}{c^2}8\pi^2\bar{\beta}^2 a_b^2 + \frac{1}{2}\frac{1}{d_0^2}\kappa\gamma_b^2\left(\frac{d_0}{d_b}\right)^{\gamma_b+2} \quad (46a)$$

$$\phi_b = \arctan\left(\frac{y_b - y}{x_b - x}\right). \quad (46b)$$

Proof: See Appendix B. ■

Note that the derived result depends only on the LoS portion. For the case without the path loss, the result in [19, eq. (35)] can be derived as $\chi_b = (1/c^2)8\pi^2\bar{\beta}^2 a_b^2$, which is the first term in (46a). Therefore, (46a) can be written in another form as

$$\chi_b = \begin{cases} \frac{1}{c^2}8\pi^2\bar{\beta}^2 a_b^2, & \text{without path loss} \\ \frac{1}{c^2}8\pi^2\bar{\beta}^2 a_b^2 + \frac{1}{2d_b^2}\gamma_b^2 a_b^2, & \text{with path loss.} \end{cases} \quad (47)$$

One can see that the values of ξ_b in both cases are the same when $\gamma_b = 0$. However, the case of no path attenuation, with $\gamma_b = 0$, does not exist in the realistic environment. Therefore, the exploration of the path loss can reduce the CRB in the wireless NLoS geolocation.

In what follows, we proceed to investigate the improved position accuracy in the hybrid model based on (45). The hybrid model is referred to as the usual time delay model using the path attenuation parameterized in (6). Substituting (2) into (6) and inserting the substituted result into (47), the CRB in (45) can be written as

$$\epsilon^2 \geq \frac{32\pi^2 f_0^2 d_0^2\sum_{b=M+1}^{B}\alpha_b}{\frac{E_s}{N_0}c^2\sum_{b_1=M+1}^{B}\sum_{b_2=M+1}^{B}\alpha_{b_1}\alpha_{b_2}\sin^2(\phi_{b_2}-\phi_{b_1})} \quad (48)$$

where α_b is given by

$$\alpha_b = \begin{cases} \frac{1}{c^2}8\pi^2\bar{\beta}^2\left(\frac{d_0}{d_b}\right)^{\gamma_b}, & \text{ordinary ToA} \\ \frac{1}{c^2}8\pi^2\bar{\beta}^2\left(\frac{d_0}{d_b}\right)^{\gamma_b} & \\ \quad +\frac{1}{2d_0^2}\gamma_b^2\left(\frac{d_0}{d_b}\right)^{\gamma_b+2}, & \text{hybrid SS}-\text{ToA.} \end{cases} \quad (49)$$

It is worth noting that the aforementioned result can be applied to a large class of signals, since we do not assume any structure of the transmitted signal $s(t)$. In [36], the estimation of the position parameter is discussed by first estimating the time delay τ_b and then recovering $\mathbf{p}$ from such a sufficient estimate. The estimator design for estimating the mobile position $\mathbf{p}$ from the ToA is beyond the scope of this paper (see, e.g., [40] for the mobile position estimation and the corresponding performance analysis). It is herein interesting to investigate the inherent accuracy limitation of the proposed hybrid method via the derived CRB.

V. Numerical Examples

The system is assumed to operate at the center frequency $f_0 = 1.9$ GHz [25]. From (1), we have

$$10\log_{10}\left(\frac{E_b}{N_0}\right) = \kappa_{\mathrm{dB}} + 10\gamma_b\log_{10}\left(\frac{d_0}{d_b}\right) + 10\log_{10}\left(\frac{E_s}{N_0}\right) \quad (50)$$

where E_s/N_0 is the transmitted SNR. In general, the term $10\log_{10}(E_b/N_0)$ can be considered as a received SNR.[2] For a simple link budget, we assume that $\gamma_b = 4.5425$, $d_0 = 100$ m, and $d_b = 1000$ m. The path loss to the bth BS is $\kappa_{\mathrm{dB}} + 10\gamma_b\log_{10}(d_0/d_b) = -123$ dB. Taking into account the path attenuation, the transmitter should transmit a high SNR, i.e., at least 123 dB so that the receiver can receive more than 0 dB. We consider the transmitted SNR instead of the received SNR because, first, the system may have different received SNRs caused by the different path losses, and second, it would be difficult to evaluate the effect of the SS information on the localization performance if the received SNR were considered.

A. Range Estimation

To investigate the ToA performance of two time delay estimators, we consider a range estimation where there are only one transmitter and one receiver. Thus, (5) can be modified as $r(t) = a(\tau_0)s(t-\tau_0) + n(t)$, with τ_0 being the time delay. In this paper, we consider the orthogonal-frequency-division-multiplexing (OFDM) signal [41], [42]. The OFDM signal of duration $t \in (0, T_s]$ is given by (see, e.g., [43])

$$\tilde{s}(t) = \sum_{k=0}^{N-1} b_k e^{j2\pi f_k t} \quad (51)$$

where $\{b_k\}_{k=0}^{N-1}$ is the block of N complex data symbols chosen from a signal constellation such as quadrature-amplitude modulation or phase-shift keying (PSK), and $f_k = f_0 + (1/T_s)k$. At the receiver, the OFDM signal is down-converted to a baseband representation, i.e., $s(t) = \tilde{s}(t)e^{-j2\pi f_0 t}$.

Lemma 1 (Effective Bandwidth of the Baseband OFDM Signal): The effective bandwidth of the baseband OFDM signal is given by

$$\bar{\beta} = \frac{1}{T_s}\sqrt{\frac{1}{6}(2N^2 - 3N + 1)}. \quad (52)$$

[2] When considering the path attenuation, such as in this paper, the received SNR is related to parameter a_b, which depends on several parameters, including κ (which again depends on d_0 and f_0), d_b, and γ. Since the effects of these parameters on the geolocation performance will be investigated in this paper, we need to adjust the value of these parameters. In this case, it is inconvenient to set the received SNR at a specific value. Therefore, in the simulations, we consider the transmitted SNR, which is defined as the ratio between the transmitted power and the noise power at the receiver, rather than the received SNR.

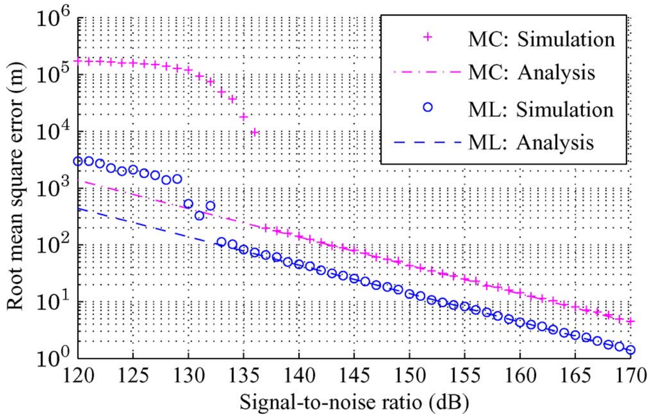

Fig. 1. RMSE of the position estimate as a function of the SNR (E_s/N_0) (in decibels) for $\gamma = 4.5425$, $d = 1000$ m, $T_s = 10^{-3}$ s, $\bar{\beta} = 3.6517 \times 10^4$ Hz, sampling time $= 3.7037 \times 10^{-9}$ s, and $N_R = 1000$ independent runs.

Proof: See Appendix C. ∎

Note that the OFDM signal in (51) used in practical systems is of limited duration. However, in Appendix C, the integration limits are evaluated in the range $(-\infty, \infty)$. Due to the periodic property of the signal in (51), this kind of extension will not affect the result of the effective bandwidth.

We employ the OFDM with $N = 2^5$ subbands. The quadrature PSK is used as the signal constellation. The theoretical root-mean-square error (RMSE) is computed from the square roots of (31b) and (42), which are multiplied by c. For the least computation, the observation period is chosen as $T = T_s + \tau_0$.

In Fig. 1, the RMSE of the estimate of the distance between the transmitter and the receiver is shown as a function of the transmitted SNR. For a low SNR, both the MC estimator and the ML estimator provide meaningless distance estimates, i.e., the RMSE is even larger than the actual distance. It can be seen that the SNR threshold, i.e., the SNR at which the ML estimator and the MC estimator merge to their asymptotic errors, respectively, is approximately 137 dB for the MC estimator and 133 dB for the ML estimator. Clearly, when the SNR is well below the threshold, the received signal is immersed in a relatively strong noise. Therefore, no reliable ranging information can be inferred from the received signal. The use of the path loss can gain an accuracy of more than 600 m for the positioning system considered here.

In Fig. 2, the RMSE is shown as a function of the signal duration T_s, which is inversely proportional to the effective bandwidth of the OFDM signal. It can be seen that when the signal duration is smaller, the RMSEs of both estimators approach the same value, i.e., $1/(E_s/N_0)8\pi^2\bar{\beta}^2 a_0^2$. For a larger signal duration, the ML estimator provides a constant RMSE, which almost does not increase with the increase of the signal duration. The cause of this phenomenon is that the time delay in this regime is mainly estimated from the SS in the path gain. From (42), the term $8\pi^2\bar{\beta}^2$ has less of an impact as the signal duration increases. The error saturation is then dominated by $(1/2\tau_0^2)\gamma^2$, which is independent of the effective bandwidth. The ML estimate has a smaller RMSE than the MC estimate. This is because the ML estimator exploits the information from the path attenuation, while the MC estimator does not use the information contained in the path gain.

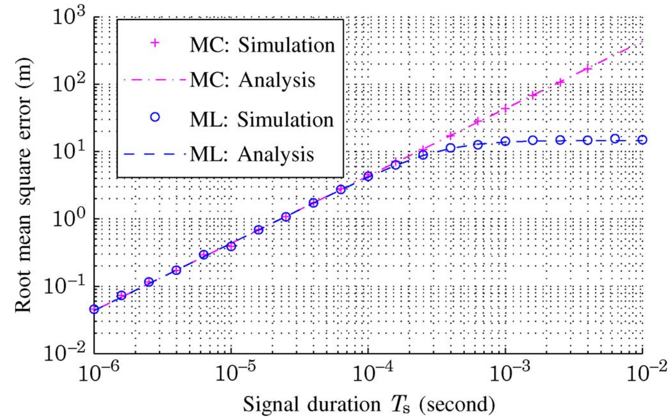

Fig. 2. RMSE of the position estimate as a function of the signal duration T_s (in seconds) for $\gamma = 4.5425$, $d = 1000$ m, $10\log_{10}(E_s/N_0) = 150$ dB, sampling time $= (1/2.5 \times 10^5)T$ s, and $N_R = 1000$ independent runs.

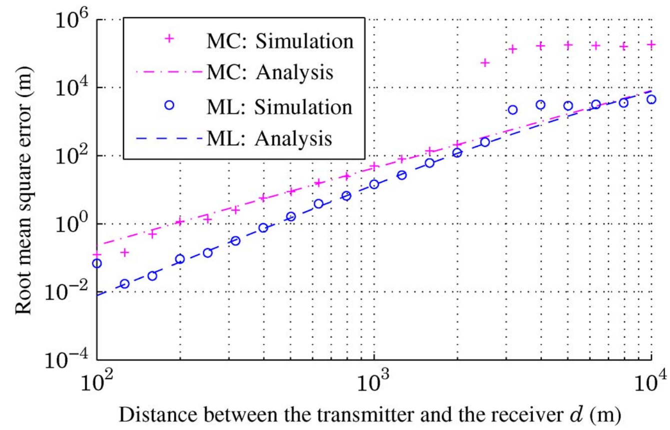

Fig. 3. RMSE of the position estimate as a function of the distance d (in meters) for $\bar{\beta} = 3.6517 \times 10^4$ Hz, $\gamma = 4.5425$, $10\log_{10}(E_s/\sigma_n^2) = 150$ dB, $T_s = 10^{-3}$ s, sampling time $= (1/2 \times 10^6)T$ s, and $N_R = 100$ independent runs.

In Fig. 3, the RMSE is shown as a function of the distance d between the transmitter and the receiver. A larger distance causes a larger estimation error. The performance improvement of the ML estimator over the MC estimator is more evident at a closer distance. In the range of large distances, the ML estimator can perform the ToA estimation for a longer distance than the MC estimator can. For a large distance, particularly for more than 1 km, the receiver receives an SNR that is lower than a necessary threshold above which the ranging information can reliably be inferred from the received signal (see the discussion about Fig. 1).

B. Cellular System

Consider a certain configuration of a cellular system with effective bandwidth $\bar{\beta}$ of $(1/\sqrt{3})5$ MHz [36]. In seven hexagonal cells, let the origin of the Cartesian coordinate lie at the center of the central cell, as illustrated in Fig. 4. The BSs are thus located at the center of each cell with the position

$$\mathbf{P} = r \begin{bmatrix} 0 & \frac{3}{2} & 0 & -\frac{3}{2} & -\frac{3}{2} & 0 & \frac{3}{2} \\ 0 & \frac{\sqrt{3}}{2} & \sqrt{3} & \frac{\sqrt{3}}{2} & -\frac{\sqrt{3}}{2} & -\sqrt{3} & -\frac{\sqrt{3}}{2} \end{bmatrix}^T \quad (53)$$

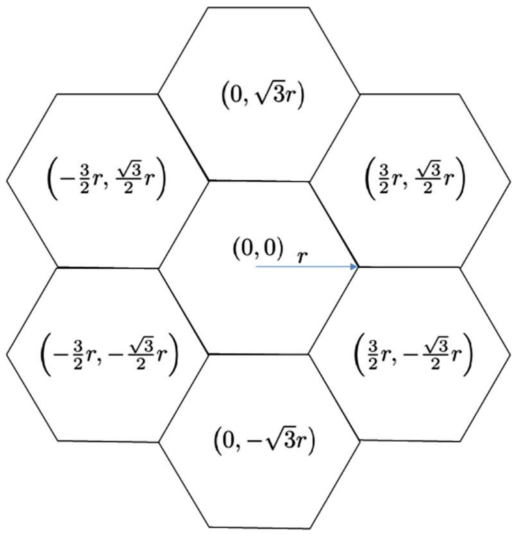

Fig. 4. Cellular system with cell radius r.

where r is the cell radius. The MS is located at $\mathbf{p} = (1/2)r \cos((1/6)\pi)[\cos((1/6)\pi)\ \sin((1/6)\pi)]^{\mathrm{T}}$ m. In what follows, we assume that the cell radius can be varied. The mobile position is $(1/4)\sqrt{3}r$ m from the center of the central cell.

With respect to the MS position, the associated angles of the BSs become

$$\boldsymbol{\phi} = \begin{bmatrix} \arctan\left(\frac{-\frac{\sqrt{3}}{8}r}{-\frac{3}{8}r}\right) \\ \arctan\left(\frac{\frac{\sqrt{3}}{2}r-\frac{\sqrt{3}}{8}r}{\frac{3}{2}r-\frac{3}{8}r}\right) \\ \arctan\left(\frac{\sqrt{3}r-\frac{\sqrt{3}}{8}r}{-\frac{3}{8}r}\right) \\ \arctan\left(\frac{\frac{\sqrt{3}}{2}r-\frac{\sqrt{3}}{8}r}{-\frac{3}{2}r-\frac{3}{8}r}\right) \\ \arctan\left(\frac{-\frac{\sqrt{3}}{2}r-\frac{\sqrt{3}}{8}r}{-\frac{3}{2}r-\frac{3}{8}r}\right) \\ \arctan\left(\frac{-\sqrt{3}r-\frac{\sqrt{3}}{8}r}{-\frac{3}{8}r}\right) \\ \arctan\left(\frac{-\frac{\sqrt{3}}{2}r-\frac{\sqrt{3}}{8}r}{\frac{3}{2}r-\frac{3}{8}r}\right) \end{bmatrix} = \begin{bmatrix} -150.0000^\circ \\ 30.0000^\circ \\ 103.8979^\circ \\ 160.8934^\circ \\ -150.0000^\circ \\ -100.8934^\circ \\ -43.8979^\circ \end{bmatrix}. \quad (54)$$

We assume that the first M BSs are subject to the NLoS signals. The positioning accuracy is calculated from the square root of (48).

In Fig. 5, the CRB is investigated as a function of the path loss exponent for several cell radii. The close-in distance $d_0 = 4$ m is chosen for indoor scenarios. We can see that the smaller the cell radius is, the better the positioning accuracy becomes. This is because the received power decreases with the increase in the distance between the MS and BSs.

In Fig. 6, the bound of positioning error is illustrated as a function of the number of the NLoS BSs for several close-in distances. The smaller the number of LoS BSs is, the worse the inherent accuracy becomes. In addition, the larger the close-in distance is, the lower the error variance becomes. It can be seen that the close-in distance has a significant impact on the inherent accuracy of the mobile position.

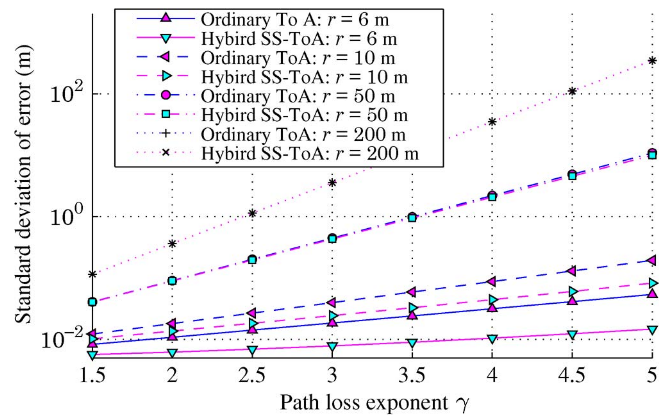

Fig. 5. Cramér–Rao lower bound as a function of the path loss exponent for several cell radii with $E_{\mathrm{s}}/N_0 = 120$ dB, $\bar{\beta} = (1/\sqrt{3})5$ MHz, $B = 7$, $M = 3$, and $d_0 = 4$ m.

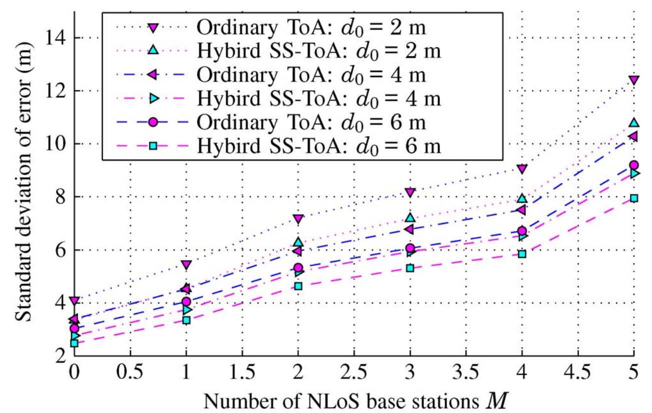

Fig. 6. Cramér–Rao lower bound as a function of the number of NLoS BSs for several close-in distances with $\bar{\beta} = (1/\sqrt{3})5$ MHz, $B = 7$, $E_{\mathrm{s}}/N_0 = 80$ dB, and $r = 20$ m.

It is shown in Figs. 5 and 6 that the position-estimation accuracy is considerably improved by using the information contained in the path loss via the developed approach.

VI. Conclusion

In this paper, we have presented an approach for hybrid wireless geolocation using the ToA in the presence of NLoS propagation by considering the additional path loss information. The MC estimator and the exact ML estimator are used to estimate the time delay. It has been shown that the ML estimator has a smaller error variance than the MC estimator. The use of the information of the path loss increases the accuracy of the ToA estimation. Numerical results illustrate that, for a low effective bandwidth of the transmitted signal, the ML estimator significantly outperforms the MC estimator. The CRB derived from the proposed method generalizes the recent result in [19] by exploring an additional term $(1/2d_0^2)\gamma_b^2(d_0/d_b)^{\gamma_b+2}$ in (49). The performance improvement is considerable, particularly for the system that invokes the signal with a small effective bandwidth, has a small distance between the MSs and BSs, and has a large value of the path loss exponent, i.e., severe path attenuation. For future work, the hybrid SS–ToA wireless NLoS geolocation based on the path attenuation can be extended to multipath scenarios [44].

APPENDIX A
DERIVATION OF JACOBIAN MATRICES $\mathbf{H}_{\rm pa}$ AND $\mathbf{H}_{\rm la}$

Let us consider

$$\frac{\partial}{\partial y}a_b = -\frac{1}{2}\frac{1}{\left(\sqrt{\left(\frac{\tilde{x}_b}{d_0}\right)^2+\left(\frac{\tilde{y}_b}{d_0}\right)^2}+\frac{l_b}{d_0}\right)^{\frac{1}{2}(\gamma_b+2)}} \times \sqrt{\kappa}\gamma_b\cos(\phi_b). \quad (55)$$

Under the same manner, we can derive

$$\frac{\partial}{\partial y}a_b = -\frac{1}{2}\frac{1}{\left(\sqrt{\left(\frac{\tilde{x}_b}{d_0}\right)^2+\left(\frac{\tilde{y}_b}{d_0}\right)^2}+\frac{l_b}{d_0}\right)^{\frac{1}{2}(\gamma_b+2)}} \times \sqrt{\kappa}\gamma_b\sin(\phi_b). \quad (56)$$

Furthermore, it can be shown that

$$\frac{\partial}{\partial l_{\acute{b}}}a_b = -\frac{1}{2}\frac{1}{d_0}\frac{1}{\left(\sqrt{\left(\frac{\tilde{x}_b}{d_0}\right)^2+\left(\frac{\tilde{y}_b}{d_0}\right)^2}+\frac{l_b}{d_0}\right)^{\frac{1}{2}(\gamma_b+2)}}\sqrt{\kappa}\gamma_b\delta_{\acute{b},b}. \quad (57)$$

According to (57), the Hessian matrix $\mathbf{H}_{\rm la}$ can be expressed, in more detail, as

$$\mathbf{H}_{\rm la} = [\mathbf{\Delta}_{\rm NL} \quad \mathbf{O}] \quad (58)$$

where $\mathbf{\Delta}_{\rm NL} \in \mathbb{R}^{M\times M}$ is a diagonal matrix whose diagonal element is given by $-(1/2)(1/d_0)(1/(\sqrt{(\tilde{x}_b/d_0)^2+(\tilde{y}_b/d_0)^2}+(l_b/d_0))^{(1/2)(\gamma_b+2)})\sqrt{\kappa}\gamma_b$. In accordance with (55) and (56), we obtain

$$\mathbf{H}_{\rm pa} = [\mathbf{H}_{\rm NL}\mathbf{\Delta}_{\rm NL} \quad \mathbf{H}_{\rm L}\mathbf{\Delta}_{\rm L}] \quad (59)$$

where $\mathbf{\Delta}_{\rm L} \in \mathbb{R}^{(B-M)\times(B-M)}$ is a diagonal matrix whose diagonal element is $-(1/2)(1/d_0)(1/(\sqrt{(\tilde{x}_b/d_0)^2+(\tilde{y}_b/d_0)^2})^{(1/2)(\gamma_b+2)})\sqrt{\kappa}\gamma_b$.

APPENDIX B
CRB DERIVATION

Let $\boldsymbol{\vartheta} \in \mathbb{R}^{(2B)\times 1}$ be the vector such that

$$\boldsymbol{\vartheta} = [\mathbf{a}^{\rm T} \quad \boldsymbol{\tau}^{\rm T}]^{\rm T} \quad (60)$$

where $\mathbf{a}$ is defined by

$$\mathbf{a} = [\,a_1 \quad a_2 \quad \cdots \quad a_B\,]^{\rm T}. \quad (61)$$

If we assign

$$\mathbf{s}_{\rm a}(t;\boldsymbol{\vartheta}) = \mathbf{A}\mathbf{s}(t;\boldsymbol{\tau}) \quad (62)$$

the received signal can be written as

$$\mathbf{r}(t) = \mathbf{s}_{\rm a}(t;\boldsymbol{\vartheta}) + \mathbf{n}(t) \quad (63)$$

where $\mathbf{s}(t;\boldsymbol{\tau})$ and $\mathbf{n}(t)$ are defined by

$$\mathbf{s}(t;\boldsymbol{\tau}) = [\,s(t-\tau_1) \quad s(t-\tau_2) \quad \cdots \quad s(t-\tau_B)\,]^{\rm T} \quad (64a)$$

$$\mathbf{n}(t) = [\,n_1(t) \quad n_2(t) \quad \cdots \quad n_B(t)\,]^{\rm T}. \quad (64b)$$

Using the chain rule, the first derivative of the log-likelihood function becomes

$$\frac{\partial}{\partial\boldsymbol{\theta}^{\rm T}}\ln\left(p\left(\mathbf{r}(t);t\in(0,T]|\boldsymbol{\theta}\right)\right) = \frac{1}{N_0}2\int_0^T(\mathbf{r}(t)-\mathbf{s}_{\rm a}(t;\boldsymbol{\vartheta}))^{\rm T}\left(\frac{\partial}{\partial\boldsymbol{\vartheta}}\mathbf{s}_{\rm a}^{\rm H}(t;\boldsymbol{\vartheta})\right)^{\rm T}dt\mathbf{H}^{\rm T} \quad (65)$$

where $\mathbf{H} = (\partial/\partial\boldsymbol{\theta})\boldsymbol{\vartheta}^{\rm T} \in \mathbb{R}^{(M+2)\times(2B)}$ is given by

$$\mathbf{H} = \begin{bmatrix} \frac{\partial}{\partial\mathbf{p}}\mathbf{a}^{\rm T} & \frac{\partial}{\partial\mathbf{p}}\boldsymbol{\tau}^{\rm T} \\ \frac{\partial}{\partial\mathbf{l}}\mathbf{a}^{\rm T} & \frac{\partial}{\partial\mathbf{l}}\boldsymbol{\tau}^{\rm T}\end{bmatrix} = \frac{1}{c}\begin{bmatrix} c\mathbf{H}_{\rm pa} & \mathbf{H}_{\rm NL} & \mathbf{H}_{\rm L} \\ c\mathbf{H}_{\rm la} & \mathbf{I} & \mathbf{O}\end{bmatrix} \quad (66)$$

with $\mathbf{H}_{\rm pa} = (\partial/\partial\mathbf{p})\mathbf{a}^{\rm T} \in \mathbb{R}^{2\times B}$ and $\mathbf{H}_{\rm la} = (\partial/\partial\mathbf{l})\mathbf{a}^{\rm T} \in \mathbb{R}^{M\times B}$ being those given in Appendix A, and $\mathbf{H}_{\rm NL} \in \mathbb{R}^{2\times M}$ and $\mathbf{H}_{\rm L} \in \mathbb{R}^{2\times(B-M)}$ being given by

$$\mathbf{H}_{\rm NL} = \begin{bmatrix}\cos(\phi_1) & \cos(\phi_2) & \cdots & \cos(\phi_M) \\ \sin(\phi_1) & \sin(\phi_2) & \cdots & \sin(\phi_M)\end{bmatrix} \quad (67a)$$

$$\mathbf{H}_{\rm L} = \begin{bmatrix}\cos(\phi_{M+1}) & \cos(\phi_{M+2}) & \cdots & \cos(\phi_B) \\ \sin(\phi_{M+1}) & \sin(\phi_{M+2}) & \cdots & \sin(\phi_B)\end{bmatrix}. \quad (67b)$$

For the second derivative, we get

$$\mathbf{J}_{\boldsymbol{\theta}\boldsymbol{\theta}} = -\mathrm{E}_{\mathbf{n}(t)}\left\{\frac{\partial^2}{\partial\boldsymbol{\theta}\partial\boldsymbol{\theta}^{\rm T}}\ln\left(p\left(\mathbf{r}(t);t\in(0,T]|\boldsymbol{\theta}\right)\right)\right\} = -\frac{1}{N_0}2\mathbf{H}\int_0^T\mathrm{E}_{\mathbf{n}(t)} \times\left\{\frac{\partial}{\partial\boldsymbol{\vartheta}}(\mathbf{r}(t)-\mathbf{s}_{\rm a}(t;\boldsymbol{\vartheta}))^{\rm T}\left(\frac{\partial}{\partial\boldsymbol{\vartheta}}\mathbf{s}_{\rm a}^{\rm H}(t;\boldsymbol{\vartheta})\right)^{\rm T}dt\right\}\mathbf{H}^{\rm T}. \quad (68)$$

Let us consider

$$\mathbf{J}_{\boldsymbol{\theta}\boldsymbol{\theta}} = -\frac{1}{N_0}2\int_0^T\mathrm{E}_{\mathbf{n}(t)}\left\{\frac{\partial}{\partial\boldsymbol{\vartheta}}\left((\mathbf{r}(t)-\mathbf{s}_{\rm a}(t;\boldsymbol{\vartheta}))^{\rm T} \times\left[\,\frac{\partial}{\partial\vartheta_1}\mathbf{s}_{\rm a}^*(t;\boldsymbol{\vartheta}) \quad \cdots \quad \frac{\partial}{\partial\vartheta_{2B}}\mathbf{s}_{\rm a}^*(t;\boldsymbol{\vartheta})\,\right]\right)\right\}dt. \quad (69)$$

For $\acute{n} \in \{1,2,\ldots,2B\}$, we obtain the column vector

$$[\mathbf{J}_{\boldsymbol{\theta}\boldsymbol{\theta}}]_{[:,\acute{n}]} = \frac{1}{N_0}2\int_0^T\left(\frac{\partial}{\partial\boldsymbol{\vartheta}}\mathbf{s}_{\rm a}^{\rm T}(t;\boldsymbol{\vartheta})\right)\frac{\partial}{\partial\vartheta_{\acute{n}}}\mathbf{s}_{\rm a}^*(t;\boldsymbol{\vartheta})dt. \quad (70)$$

Substituting (70) into (69) yields the FIM

$$\mathbf{J}_{\boldsymbol{\theta\theta}} = \frac{1}{N_0} 2 \int_0^T \left(\frac{\partial}{\partial \boldsymbol{\vartheta}} \mathbf{s}_{\mathrm{a}}^{\mathrm{T}}(t;\boldsymbol{\vartheta}) \right) \left(\frac{\partial}{\partial \boldsymbol{\vartheta}} \mathbf{s}_{\mathrm{a}}^{\mathrm{H}}(t;\boldsymbol{\vartheta}) \right)^{\mathrm{T}} dt. \quad (71)$$

Furthermore, we can derive

$$\begin{aligned} \frac{\partial}{\partial \boldsymbol{\vartheta}} \mathbf{s}_{\mathrm{a}}^{\mathrm{T}}(t;\boldsymbol{\tau}) &= \begin{bmatrix} \frac{\partial}{\partial \mathbf{a}} \left(\mathbf{s}^{\mathrm{T}}(t;\boldsymbol{\tau}) \mathbf{A}^{\mathrm{T}} \right) \\ \left(\frac{\partial}{\partial \boldsymbol{\tau}} \mathbf{s}^{\mathrm{T}}(t;\boldsymbol{\tau}) \right) \mathbf{A}^{\mathrm{T}} \end{bmatrix} \\ &= \begin{bmatrix} \frac{\partial}{\partial \mathbf{a}} \sum_{b=1}^{B} \mathbf{a}_b^{\mathrm{T}} s(t-\tau_b) \\ \left(\frac{\partial}{\partial \boldsymbol{\tau}} \mathbf{s}^{\mathrm{T}}(t;\boldsymbol{\tau}) \right) \mathbf{A}^{\mathrm{T}} \end{bmatrix} \end{aligned} \quad (72)$$

where $\mathbf{a}_b$ is the bth column of $\mathbf{A}$. Plugging (72) into (71), we obtain (73), shown at the bottom of the page. Employing the chain rule, we have (74), shown at the bottom of the page. Indeed, we can derive

$$\begin{aligned} \frac{\partial}{\partial \mathbf{a}} \left(\mathbf{s}^{\mathrm{T}}(t;\boldsymbol{\tau}) \mathbf{A}^{\mathrm{T}} \right) &= \frac{\partial}{\partial \mathbf{a}} \sum_{b=1}^{B} \mathbf{a}_b^{\mathrm{T}} s(t-\tau_b) \\ &= \begin{bmatrix} s(t-\tau_1) & \cdots & 0 \\ \vdots & \ddots & \vdots \\ 0 & \cdots & s(t-\tau_B) \end{bmatrix}. \end{aligned} \quad (75)$$

Let us consider

$$\mathbf{J}_{\boldsymbol{\theta\theta}} = \begin{bmatrix} \mathbf{J}_{\mathbf{aa}} & \mathbf{J}_{\mathbf{a}\boldsymbol{\tau}} \\ \mathbf{J}_{\boldsymbol{\tau}\mathbf{a}} & \mathbf{J}_{\boldsymbol{\tau\tau}} \end{bmatrix}$$

where $\mathbf{J}_{\mathbf{aa}}$, $\mathbf{J}_{\mathbf{a}\boldsymbol{\tau}}$, and $\mathbf{J}_{\boldsymbol{\tau\tau}}$ are

$$\begin{aligned} \mathbf{J}_{\mathbf{aa}} &= \frac{1}{N_0} 2 \int_0^T \left(\frac{\partial}{\partial \mathbf{a}} \mathbf{s}^{\mathrm{T}}(t;\boldsymbol{\tau}) \mathbf{A}^{\mathrm{T}} \right) \left(\frac{\partial}{\partial \mathbf{a}} \mathbf{s}^{\mathrm{H}}(t;\boldsymbol{\tau}) \mathbf{A}^{\mathrm{T}} \right)^{\mathrm{T}} dt \\ &= \frac{E_{\mathrm{s}}}{N_0} 2\mathbf{I} \end{aligned} \quad (76a)$$

$$\begin{aligned} \mathbf{J}_{\mathbf{a}\boldsymbol{\tau}} &= \frac{1}{N_0} 2 \int_0^T \left(\frac{\partial}{\partial \mathbf{a}} \mathbf{s}^{\mathrm{T}}(t;\boldsymbol{\tau}) \mathbf{A}^{\mathrm{T}} \right) \mathbf{A} \left(\frac{\partial}{\partial \boldsymbol{\tau}} \mathbf{s}^{\mathrm{H}}(t;\boldsymbol{\tau}) \right)^{\mathrm{T}} dt \\ &= \frac{1}{N_0} 2 \int_0^{T_{\mathrm{s}}} s(t) \frac{\partial}{\partial t} s^*(t) dt \mathbf{A} \\ &= \mathbf{O} \end{aligned} \quad (76b)$$

$$\begin{aligned} \mathbf{J}_{\boldsymbol{\tau\tau}} &= \frac{1}{N_0} 2 \int_0^T \left(\frac{\partial}{\partial \boldsymbol{\tau}} \mathbf{s}^{\mathrm{T}}(t;\boldsymbol{\tau}) \right) \mathbf{A}^{\mathrm{T}} \mathbf{A} \left(\frac{\partial}{\partial \boldsymbol{\tau}} \mathbf{s}^{\mathrm{H}}(t;\boldsymbol{\tau}) \right)^{\mathrm{T}} dt \\ &= \frac{1}{N_0} \frac{\int_{-\infty}^{\infty} f^2 \left| S(f) \right|^2 df}{\int_{-\infty}^{\infty} \left| S(f) \right|^2 df} 8\pi^2 \int_0^{T_{\mathrm{s}}} \left| s(t) \right|^2 dt \mathbf{A}^2 \\ &= \frac{E_{\mathrm{s}}}{N_0} 8\pi^2 \bar{\beta}^2 \mathbf{A}^2. \end{aligned} \quad (76c)$$

Therefore, $\mathbf{J}_{\boldsymbol{\theta\theta}}$ can be written as

$$\mathbf{J}_{\boldsymbol{\theta\theta}} = \frac{E_{\mathrm{s}}}{N_0} 2 \begin{bmatrix} \mathbf{I} & \mathbf{O} & \mathbf{O} \\ \mathbf{O} & 4\pi^2 \bar{\beta}^2 \mathbf{A}_{\mathrm{NL}}^2 & \mathbf{O} \\ \mathbf{O} & \mathbf{O} & 4\pi^2 \bar{\beta}^2 \mathbf{A}_{\mathrm{L}}^2 \end{bmatrix} \quad (77)$$

where $\mathbf{A}$ is partitioned into

$$\mathbf{A} = \begin{bmatrix} \mathbf{A}_{\mathrm{NL}} & \mathbf{O} \\ \mathbf{O} & \mathbf{A}_{\mathrm{L}} \end{bmatrix} \quad (78)$$

with $\mathbf{A}_{\mathrm{NL}}$ and $\mathbf{A}_{\mathrm{L}}$ composed of the first M and last $B-M$ diagonal elements of $\mathbf{A}$, respectively. Simple algebra yields (79), shown at the bottom of the next page.

Using the block matrix inversion lemma, we can obtain

$$\begin{aligned} \left[\mathbf{J}_{\boldsymbol{\theta\theta}}^{-1} \right]_{[2\times 2]} = \frac{1}{\frac{E_{\mathrm{s}}}{N_0} 2} c^2 \Big(& \left(c^2 \mathbf{H}_{\mathrm{pa}} \mathbf{H}_{\mathrm{pa}}^{\mathrm{T}} + 4\pi^2 \bar{\beta}^2 \mathbf{H}_{\mathrm{NL}} \mathbf{A}_{\mathrm{NL}}^2 \mathbf{H}_{\mathrm{NL}}^{\mathrm{T}} \right. \\ & \left. + 4\pi^2 \bar{\beta}^2 \mathbf{H}_{\mathrm{L}} \mathbf{A}_{\mathrm{L}}^2 \mathbf{H}_{\mathrm{L}}^{\mathrm{T}} \right) \\ & - \left(c^2 \mathbf{H}_{\mathrm{pa}} \mathbf{H}_{\mathrm{la}}^{\mathrm{T}} + 4\pi^2 \bar{\beta}^2 \mathbf{H}_{\mathrm{NL}} \mathbf{A}_{\mathrm{NL}}^2 \right) \\ & \times \left(c^2 \mathbf{H}_{\mathrm{la}} \mathbf{H}_{\mathrm{la}}^{\mathrm{T}} + 4\pi^2 \bar{\beta}^2 \mathbf{A}_{\mathrm{NL}}^2 \right)^{-1} \\ & \times \left(c^2 \mathbf{H}_{\mathrm{la}} \mathbf{H}_{\mathrm{pa}}^{\mathrm{T}} + 4\pi^2 \bar{\beta}^2 \mathbf{A}_{\mathrm{NL}}^2 \mathbf{H}_{\mathrm{NL}}^{\mathrm{T}} \right) \Big)^{-1}. \end{aligned} \quad (80)$$

Substituting (58) into $(c^2 \mathbf{H}_{\mathrm{la}} \mathbf{H}_{\mathrm{la}}^{\mathrm{T}} + 4\pi^2 \bar{\beta}^2 \mathbf{A}_{\mathrm{NL}}^2)^{-1}$ in (80), we obtain

$$\begin{aligned} & \left(c^2 \mathbf{H}_{\mathrm{la}} \mathbf{H}_{\mathrm{la}}^{\mathrm{T}} + 4\pi^2 \bar{\beta}^2 \mathbf{A}_{\mathrm{NL}}^2 \right)^{-1} \\ & \quad = \left(4\pi^2 \bar{\beta}^2 \mathbf{A}_{\mathrm{NL}}^2 + c^2 [\boldsymbol{\Delta}_{\mathrm{NL}} \quad \mathbf{O}] \begin{bmatrix} \boldsymbol{\Delta}_{\mathrm{NL}} \\ \mathbf{O} \end{bmatrix} \right)^{-1} \\ & \quad = \tilde{\boldsymbol{\Lambda}}_{\mathrm{NL}}^{-1} \end{aligned} \quad (81)$$

$$\mathbf{J}_{\boldsymbol{\theta\theta}} = \frac{1}{N_0} 2 \int_0^T \begin{bmatrix} \left(\frac{\partial}{\partial \mathbf{a}} \mathbf{s}^{\mathrm{T}}(t;\boldsymbol{\tau}) \mathbf{A}^{\mathrm{T}} \right) \left(\frac{\partial}{\partial \mathbf{a}} \mathbf{s}^{\mathrm{H}}(t;\boldsymbol{\tau}) \mathbf{A}^{\mathrm{T}} \right)^{\mathrm{T}} & \left(\frac{\partial}{\partial \mathbf{a}} \mathbf{s}^{\mathrm{T}}(t;\boldsymbol{\tau}) \mathbf{A}^{\mathrm{T}} \right) \mathbf{A} \left(\frac{\partial}{\partial \boldsymbol{\tau}} \mathbf{s}^{\mathrm{H}}(t;\boldsymbol{\tau}) \right)^{\mathrm{T}} \\ \left(\frac{\partial}{\partial \boldsymbol{\tau}} \mathbf{s}^{\mathrm{T}}(t;\boldsymbol{\tau}) \right) \mathbf{A}^{\mathrm{T}} \left(\frac{\partial}{\partial \mathbf{a}} \mathbf{s}^{\mathrm{H}}(t;\boldsymbol{\tau}) \mathbf{A}^{\mathrm{T}} \right)^{\mathrm{T}} & \left(\frac{\partial}{\partial \boldsymbol{\tau}} \mathbf{s}^{\mathrm{T}}(t;\boldsymbol{\tau}) \right) \mathbf{A}^{\mathrm{T}} \mathbf{A} \left(\frac{\partial}{\partial \boldsymbol{\tau}} \mathbf{s}^{\mathrm{H}}(t;\boldsymbol{\tau}) \right)^{\mathrm{T}} \end{bmatrix} dt \quad (73)$$

$$\frac{\partial}{\partial \boldsymbol{\tau}} \mathbf{s}^{\mathrm{T}}(t;\boldsymbol{\tau}) = - \begin{bmatrix} \frac{\partial}{\partial t} s(t) & \frac{\partial}{\partial t} s\left(t-(\tau_2-\tau_1)\right) & \cdots & \frac{\partial}{\partial t} s\left(t-(\tau_B-\tau_1)\right) \\ \frac{\partial}{\partial t} s\left(t-(\tau_1-\tau_2)\right) & \frac{\partial}{\partial t} s(t) & \cdots & \frac{\partial}{\partial t} s\left(t-(\tau_B-\tau_2)\right) \\ \vdots & \vdots & \ddots & \vdots \\ \frac{\partial}{\partial t} s\left(t-(\tau_1-\tau_B)\right) & \frac{\partial}{\partial t} s\left(t-(\tau_2-\tau_B)\right) & \cdots & \frac{\partial}{\partial t} s(t) \end{bmatrix} \quad (74)$$

where $\tilde{\mathbf{\Lambda}}_{\mathrm{NL}} = 4\pi^2\bar{\beta}^2\mathbf{A}_{\mathrm{NL}}^2 + c^2\mathbf{\Delta}_{\mathrm{NL}}^2$. Inserting (59) into $\mathbf{H}_{\mathrm{pa}}\mathbf{H}_{\mathrm{pa}}^{\mathrm{T}}$ yields

$$\mathbf{H}_{\mathrm{pa}}\mathbf{H}_{\mathrm{pa}}^{\mathrm{T}} = \mathbf{H}_{\mathrm{NL}}\mathbf{\Delta}_{\mathrm{NL}}^2\mathbf{H}_{\mathrm{NL}}^{\mathrm{T}} + \mathbf{H}_{\mathrm{L}}\mathbf{\Delta}_{\mathrm{L}}^2\mathbf{H}_{\mathrm{L}}^{\mathrm{T}}. \tag{82}$$

Plugging (58) and (59) into $\mathbf{H}_{\mathrm{la}}\mathbf{H}_{\mathrm{pa}}^{\mathrm{T}}$, we obtain

$$\mathbf{H}_{\mathrm{la}}\mathbf{H}_{\mathrm{pa}}^{\mathrm{T}} = \mathbf{\Delta}_{\mathrm{NL}}^2\mathbf{H}_{\mathrm{NL}}^{\mathrm{T}}. \tag{83}$$

Define $\tilde{\mathbf{\Lambda}}_{\mathrm{L}} = 4\pi^2\bar{\beta}^2\mathbf{A}_{\mathrm{L}}^2 + c^2\mathbf{\Delta}_{\mathrm{L}}^2$. Substituting (81)–(83) into (80), we obtain

$$\begin{aligned}
&\left[\mathbf{J}_{\boldsymbol{\theta\theta}}^{-1}\right]_{[2\times 2]} \\
&= \frac{1}{\frac{E_s}{N_0}2}c^2\Bigg(\Big(c^2\left(\mathbf{H}_{\mathrm{NL}}\mathbf{\Delta}_{\mathrm{NL}}^2\mathbf{H}_{\mathrm{NL}}^{\mathrm{T}} + \mathbf{H}_{\mathrm{L}}\mathbf{\Delta}_{\mathrm{L}}^2\mathbf{H}_{\mathrm{L}}^{\mathrm{T}}\right) \\
&\qquad + 4\pi^2\bar{\beta}^2\mathbf{H}_{\mathrm{NL}}\mathbf{A}_{\mathrm{NL}}^2\mathbf{H}_{\mathrm{NL}}^{T} + 4\pi^2\bar{\beta}^2\mathbf{H}_{\mathrm{L}}\mathbf{A}_{\mathrm{L}}^2\mathbf{H}_{\mathrm{L}}^{\mathrm{T}}\Big) \\
&\qquad - \left(c^2\mathbf{H}_{\mathrm{NL}}\mathbf{\Delta}_{\mathrm{NL}}^2 + 4\pi^2\bar{\beta}^2\mathbf{H}_{\mathrm{NL}}\mathbf{A}_{NL}^2\right)\tilde{\Lambda}_{\mathrm{NL}}^{-1} \\
&\qquad \times \left(c^2\mathbf{\Delta}_{\mathrm{NL}}^{T}\mathbf{H}_{\mathrm{NL}}^{\mathrm{T}} + 4\pi^2\tilde{\beta}\mathbf{A}_{\mathrm{NL}}^2\mathbf{H}_{\mathrm{NL}}^{\mathrm{T}}\right)\Bigg)^{-1} \\
&= \frac{1}{\frac{E_s}{N_0}2}c^2\left(\mathbf{H}_{\mathrm{L}}\tilde{\mathbf{\Lambda}}_{\mathrm{L}}\mathbf{H}_{\mathrm{L}}^{\mathrm{T}}\right)^{-1} \\
&= \left(\sum_{b=M+1}^{B}\nu_b\begin{bmatrix}\cos^2(\phi_b) & \sin(\pi_b)\cos(\phi_b)\\ \sin(\phi_b)\cos(\phi_b) & \sin^2(\phi_b)\end{bmatrix}\right)^{-1}
\end{aligned} \tag{84}$$

where ν_b is given by

$$\nu_b = \frac{E_s}{N_0}\left(\frac{1}{c^2}8\pi^2\bar{\beta}^2a_b^2 + \frac{1}{2}\frac{1}{d_0^2}\frac{1}{\left(\sqrt{\left(\frac{\tilde{x}_b}{d_0}\right)^2+\left(\frac{\tilde{y}_b}{d_0}\right)^2}\right)^{\gamma_b+2}}\kappa\gamma_b^2\right). \tag{85}$$

Let us introduce $[\mathbf{J}_{\boldsymbol{\theta\theta}}^{-1}]_{[2\times 2]}$ as

$$\begin{aligned}
[\mathbf{J}_{\boldsymbol{\theta\theta}}^{-1}]_{[2\times 2]} &= \begin{bmatrix} a_{11} & a_{12}\\ a_{21} & a_{22}\end{bmatrix}^{-1} \\
&= \frac{1}{a_{11}a_{22} - a_{12}a_{21}}\begin{bmatrix} a_{22} & -a_{12}\\ -a_{21} & a_{11}\end{bmatrix}
\end{aligned} \tag{86}$$

where a_{11}, a_{12}, a_{21}, and a_{22} are given by

$$a_{11} = \sum_{b=M+1}^{B}\nu_b\cos^2(\phi_b) \tag{87a}$$

$$a_{12} = \sum_{b=M+1}^{B}\nu_b\sin(\phi_b)\cos(\phi_b) \tag{87b}$$

$$a_{21} = \sum_{b=M+1}^{B}\nu_b\sin(\phi_b)\cos(\phi_b) \tag{87c}$$

$$a_{22} = \sum_{b=M+1}^{B}\nu_b\sin^2(\phi_b). \tag{87d}$$

The total positioning accuracy of both axes is given by

$$\epsilon^2 \geq \mathrm{tr}\left([\mathbf{J}_{\boldsymbol{\theta\theta}}^{-1}]_{[2\times 2]}\right) = \frac{2\sum\limits_{b=M+1}^{B}\nu_b}{\sum\limits_{b_1=M+1}^{B}\sum\limits_{b_2=M+1}^{B}\nu_{b_1}\nu_{b_2}\sin^2(\phi_{b_2}-\phi_{b_1})} \tag{88}$$

which gives the result in (45).

Appendix C
Effective Bandwidth of the Baseband OFDM Signal

Using Parseval's theorem, the signal energy is given by

$$\begin{aligned}
\int_{-\infty}^{\infty}\left|\tilde{S}(f)\right|^2 df &= \int_{-\infty}^{\infty}|\tilde{s}(t)|^2\,dt \\
&= \sum_{k_1=0}^{N-1}\sum_{k_2=0}^{N-1}b_{k_1}b_{k_2}^{*}\lim_{T_\infty\to\infty}2T_\infty \\
&\quad \times \mathrm{sinc}\left(\frac{1}{T_s}2\pi(k_1-k_2)T_\infty\right).
\end{aligned} \tag{89}$$

From the derivative property of the Fourier transform, the second moment of the signal frequency reads as

$$\begin{aligned}
\int_{-\infty}^{\infty}f^2\left|\tilde{S}(f)\right|^2 df &= \frac{1}{4\pi^2}\int_{-\infty}^{\infty}\left|\frac{\partial}{\partial t}\tilde{s}(t)\right|^2 dt \\
&= \sum_{k_1=0}^{N-1}\sum_{k_2=0}^{N-1}b_{k_1}b_{k_2}^{*}f_{k_1}f_{k_2} \\
&\quad \times \lim_{T_\infty\to\infty}2T_\infty\mathrm{sinc}\left(\frac{1}{T_s}2\pi(k_1-k_2)T_\infty\right).
\end{aligned} \tag{90}$$

$$\mathbf{J}_{\boldsymbol{\theta\theta}} = \frac{1}{c^2}\frac{E_s}{N_0}2\begin{bmatrix} c^2\mathbf{H}_{\mathrm{pa}}\mathbf{H}_{\mathrm{pa}}^{\mathrm{T}} + 4\pi^2\bar{\beta}^2\mathbf{H}_{\mathrm{NL}}\mathbf{A}_{\mathrm{NL}}^2\mathbf{H}_{\mathrm{NL}}^{\mathrm{T}} + 4\pi^2\bar{\beta}^2\mathbf{H}_{\mathrm{L}}\mathbf{A}_{\mathrm{L}}^2\mathbf{H}_{\mathrm{L}}^{\mathrm{T}} & c^2\mathbf{H}_{\mathrm{pa}}\mathbf{H}_{\mathrm{la}}^{\mathrm{T}} + 4\pi^2\bar{\beta}^2\mathbf{H}_{\mathrm{NL}}\mathbf{A}_{\mathrm{NL}}^2 \\ c^2\mathbf{H}_{\mathrm{la}}\mathbf{H}_{\mathrm{pa}}^{\mathrm{T}} + 4\pi^2\bar{\beta}^2\mathbf{A}_{\mathrm{NL}}^2\mathbf{H}_{\mathrm{NL}}^{\mathrm{T}} & c^2\mathbf{H}_{\mathrm{la}}\mathbf{H}_{\mathrm{la}}^{\mathrm{T}} + 4\pi^2\bar{\beta}^2\mathbf{A}_{\mathrm{NL}}^2\end{bmatrix} \tag{79}$$

The square of the effective bandwidth can be written as

$$\bar{\beta}^2 = \lim_{T_\infty \to \infty} \frac{\sum_{k_1=0}^{N-1}\sum_{k_2=0}^{N-1} f_{k_1} f_{k_2} b_{k_1} b_{k_2}^* \operatorname{sinc}\left(\frac{1}{T_s} 2\pi (k_1 - k_2) T_\infty\right)}{\sum_{k_1=0}^{N-1}\sum_{k_2=0}^{N-1} b_{k_1} b_{k_2}^* \operatorname{sinc}\left(\frac{1}{T_s} 2\pi (k_1 - k_2) T_\infty\right)}. \tag{91}$$

Using $\operatorname{sinc}(\infty) = 0$ and $|b_k|^2 = |b_{\acute{k}}|^2; k \neq \acute{k}$, the effective bandwidth of the OFDM signal is given by

$$\bar{\beta} = \sqrt{f_0^2 + \frac{1}{T_s}(N-1)\left(f_0 + \frac{1}{6T_s}(2N-1)\right)} \tag{92}$$

which reduces to (52) for the baseband OFDM system.

References

[1] B. Hofmann-Wellenhof, H. Lichtenegger, and J. Collins, *Global Positioning System: Theory and Practice*, 4th ed. New York: Springer-Verlag, 1997.

[2] J. Caffery, *Wireless Location in CDMA Cellular Radio System*. Norwell, MA: Kluwer, 1999.

[3] K. Pahlavan, P. Krishnamurthy, and J. Beneat, "Wideband radio propagation modeling for indoor geolocation applications," *IEEE Commun. Mag.*, vol. 36, no. 4, pp. 60–65, Apr. 1998.

[4] K. Pahlavan, X. Li, and J.-P. Mäkelä, "Indoor geolocation science and technology," *IEEE Commun. Mag.*, vol. 40, no. 2, pp. 112–118, Feb. 2002.

[5] S. S. Soliman and C. E. Wheatley, "Geolocation technologies and applications for third generation wireless," *Wireless Commun. Comput.*, vol. 2, no. 3, pp. 229–251, May 2002.

[6] G. L. Stüber and J. Caffery, Jr., "Radiolocation techniques," in *The Mobile Communications Handbook,* 2nd ed., J. Gibson, Ed. Boca Raton, FL: CRC, Apr. 2000, ch. 24.

[7] S. Gezici, Z. Tian, G. B. Giannakis, H. Kobayashi, A. F. Molisch, H. V. Poor, and Z. Sahinoglu, "Localization via ultra-wideband radios: A look at positioning aspects for future sensor networks," *IEEE Signal Process. Mag.*, vol. 22, no. 4, pp. 70–84, Jul. 2005.

[8] R. Roberts, "Ranging subcommittee final report," Harris Corporation, Melbourne, FL, Tech. Rep., Nov. 2004. [Online]. Available: http://grouper.ieee.org/groups/802/15/pub/04/15-04-0581-07.25-004a-ranging-subcommittee-final-report.doc

[9] T. S. Rappaport, J. H. Reed, and B. D. Woerner, "Position location using wireless communications on highways of the future," *IEEE Commun. Mag.*, vol. 34, no. 10, pp. 33–41, Oct. 1996.

[10] J. J. Caffery, Jr. and G. L. Stüber, "Overview of radiolocation in CDMA cellular systems," *IEEE Commun. Mag.*, vol. 36, no. 4, pp. 38–45, Apr. 1998.

[11] N. A. Alsindi, B. Alavi, and K. Pahlavan, "Measurement and modeling of ultrawideband TOA-based ranging in indoor multipath environments," *IEEE Trans. Veh. Technol.*, vol. 58, no. 3, pp. 1046–1058, Mar. 2009.

[12] S. Venkatraman, J. Caffery, Jr., and H.-R. You, "A novel ToA location algorithm using LoS range estimation for NLoS environments," *IEEE Trans. Veh. Technol.*, vol. 53, no. 5, pp. 1515–1524, Sep. 2004.

[13] S. Al-Jazzar, M. Ghogho, and D. McLernon, "A joint TOA/AOA constrained minimization method for locating wireless devices in non-line-of-sight environment," *IEEE Trans. Veh. Technol.*, vol. 58, no. 1, pp. 468–472, Jan. 2009.

[14] S. Mazuelas, F. A. Lago, J. Blas, A. Bahillo, P. Fernandez, R. M. Lorenzo, and E. J. Abril, "Prior NLOS measurement correction for positioning in cellular wireless networks," *IEEE Trans. Veh. Technol.*, vol. 58, no. 5, pp. 2585–2591, Jun. 2009.

[15] H. Cramér, "A contribution to the theory of statistical estimation," *Skand. Akt. Tidskr.*, vol. 29, pp. 85–94, 1945.

[16] C. R. Rao, "Information and accuracy attainable in the estimation of statistical parameters," *Bull. Calcutta Math. Soc.*, vol. 37, pp. 81–91, 1945.

[17] C. R. Rao, "Minimum variance and the estimation of several parameters," *Math. Proc. Camb. Philos. Soc.*, vol. 43, no. 2, pp. 280–283, Apr. 1947.

[18] R. A. Fisher, "On the mathematical foundations of theoretical statistics," *Philos. Trans. Roy. Soc. London Ser. A*, vol. 222, pp. 309–368, 1922.

[19] Y. Qi, H. Kobayashi, and H. Suda, "Analysis of wireless geolocation in a non-line-of-sight environment," *IEEE Trans. Wireless Commun.*, vol. 5, no. 3, pp. 672–681, Mar. 2006.

[20] A. Catovic and Z. Sahinoglu, "The Cramér-Rao bounds of hybrid TOA/RSS and TDOA/RSS location estimation schemes," *IEEE Commun. Lett.*, vol. 8, no. 10, pp. 626–628, Oct. 2004.

[21] J.-Y. Huang and Q. Wan, "Comments on 'the Cramér-Rao bounds of hybrid TOA/RSS and TDOA/RSS location estimation schemes'," *IEEE Commun. Lett.*, vol. 11, no. 11, pp. 848–849, Nov. 2007.

[22] B.-C. Liu and K.-H. Lin, "Cellular geolocation employing hybrid of relative signal strength and propagation delay," in *Proc. IEEE WCNC*, Las Vegas, NV, Apr. 2006, vol. 43, pp. 280–283.

[23] A. Goldsmith, *Wireless Communications*. New York: Cambridge Univ. Press, 2005.

[24] T. S. Rappaport, *Wireless Communications: Principle and Practice*, 2nd ed. Englewood Cliffs, NJ: Prentice-Hall, 2002.

[25] V. Erceg, L. J. Greenstein, S. Y. Tjandra, S. R. Parkoff, A. Gupta, B. Kulic, A. A. Julius, and R. Bianchi, "An empirically based path loss model for wireless channels in suburban environments," *IEEE J. Sel. Areas Commun.*, vol. 17, no. 7, pp. 1205–1211, Jul. 1999.

[26] J. Borràs, P. Hatrack, and N. B. Manclayam, "Decision theoretic framework for NLOS identification," in *Proc. IEEE VTC*, Ottawa, ON, Canada, May 1998, vol. 2, pp. 1583–1587.

[27] K. Yu and Y. J. Guo, "Statistical NLOS identification based on AOA, TOA and signal strength," *IEEE Trans. Veh. Technol.*, vol. 58, no. 1, pp. 274–286, Jan. 2009.

[28] B. Sklar, *Digital Communications: Fundamentals and Applications*, 2nd ed. Upper Saddle River, NJ: Prentice-Hall, 2001.

[29] R. E. Collins, *Antennas and Radiowave Propagation*. Singapore: McGraw-Hill, 1985.

[30] C. A. Balanis, *Antenna Theory*. New York: Wiley, 1997.

[31] E. A. Lee and D. G. Messerschmitt, *Digital Communications*, 2nd ed. Norwell, MA: Kluwer, 1999.

[32] W. R. Madych, "Solutions of underdetermined systems of linear equations," in *Spatial Statistics and Imaging: Papers From the Research Conference on Image Analysis and Spatial Statistics Held at Bowdoin College, Brunswick, Maine, Summer 1988*, ser. Lecture Notes-Monograph Series, vol. 20, A. Possolo, Ed. Hayward, CA: Inst. Math. Statist., 1991, pp. 227–238.

[33] C. W. Helstrom, *Elements of Signal Detection and Estimation*. Englewood Cliffs, NJ: Prentice-Hall, 1995.

[34] H. V. Poor, *An Introduction to Signal Detection and Estimation*, 2nd ed. New York: Springer-Verlag, 1994.

[35] H. L. Van Trees, *Detection, Estimation, and Modulation Theory, Part I: Detection, Estimation, and Linear Modulation Theory*. New York: Wiley, 2001.

[36] Y. Qi, "Wireless geolocation in a non-line-sight environment," Ph.D. dissertation, Princeton Univ., Princeton, NJ, Nov. 2003.

[37] H. Urkowitz, *Signal Theory and Random Process*. Norwell, MA: Artech House, 1983.

[38] L. Ljung, *System Identification: Theory for the User*. Englewood Cliffs, NJ: Prentice-Hall, 1987.

[39] R. N. McDonough and A. D. Whalen, *Detection of Signals in Noise*, 2nd ed. New York: Academic, 1995.

[40] B. Tau Sieskul, F. Zheng, and T. Kaiser, "A hybrid SS-ToA wireless NLoS geolocation based on path attenuation: Mobile position estimation," in *Proc. IEEE WCNC*, Budapest, Hungary, Apr. 2009, pp. 1–6.

[41] H. F. Harmuth, "On the transmission of information by orthogonal time functions," *Trans. AIEE Pt. I Commun. Electron.*, vol. 79, pp. 248–255, Jul. 1960.

[42] R. W. Chang, "Synthesis of band-limited orthogonal signals for multichannel data transmission," *Bell Syst. Tech. J.*, vol. 45, pp. 1775–1796, Dec. 1960.

[43] T. Hwang, C. Yang, G. Wu, S. Li, and G. Y. Li, "OFDM and its wireless applications: A survey," *IEEE Trans. Veh. Technol.*, vol. 58, no. 4, pp. 1673–1694, May 2009.

[44] Y. Qi, H. Kobayashi, and H. Suda, "On time-of-arrival positioning in a multipath environment," *IEEE Trans. Veh. Technol.*, vol. 55, no. 5, pp. 1516–1526, Sep. 2006.

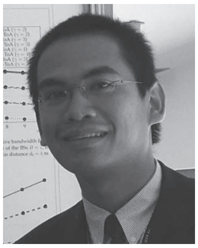

Bamrung Tau Sieskul (S'05) was born in Lopburi, Thailand, in 1979. He received the B.Eng. and M.Eng. degrees in electrical engineering from Chulalongkorn University, Bangkok, Thailand, in 2002 and 2004, respectively. He is currently working the Ph.D. degree in electrical engineering, under the supervision of Prof. T. Kaiser, with the Institute of Communication Technology, Faculty of Electrical Engineering and Computer Science, Leibniz University Hannover, Hanover, Germany.

In April and May in 2001, he was a Summer Intern with the IBM Thailand Company, Ltd., Bangkok. From 2002 to 2004, he was a Research Assistant with the Department of Electrical Engineering, Chulalongkorn University, Bangkok. From 2005 to 2006, he was a Scientific Assistant with the Department of Communication Engineering, University of Duisburg-Essen, Duisburg, Germany. He is the author of several articles in conference proceedings and journals and of a book chapter. He regularly serves as a Reviewer for conference proceedings and journals. His interests began with direction-of-arrival estimation, antenna array, and linear algebra. Currently, his research lies in the area of signal processing for wireless communications, including estimation bounds, multiantennas, channel modeling, channel capacity, and ultrawideband.

Mr. Tau Sieskul was listed in the *Marquis Who's Who in the World* in 2007.

Feng Zheng (SM'06) received the B.Sc. and M.Sc. degrees in electrical engineering from Xidian University, Xi'an, China, in 1984 and 1987, respectively, and the Ph.D. degree in automatic control from the Beijing University of Aeronautics and Astronautics, Beijing, China, in 1993.

Previously, he held an Alexander von Humboldt Research Fellowship with the University of Duisburg, Duisburg, Germany, and research positions with Tsinghua University, Beijing, the National University of Singapore, Singapore, and the University of Limerick, Limerick, Ireland. From 1995 to 1998, he was with the Center for Space Science and Applied Research, Chinese Academy of Sciences, Beijing, as an Associate Professor. Since July 2007, he has been with the Institute of Communication Technology, Faculty of Electrical Engineering and Computer Science, Leibniz University Hannover, Hannover, Germany, as a Wissenschaftlicher Beirat. His research interests are in the areas of ultrawideband multiple-input–multiple-output wireless communications, signal processing, and systems and control theory.

Dr. Zheng is a corecipient of several awards, including the National Natural Science Award in 1999 from the Chinese Government, the Science and Technology Achievement Award in 1997 from the State Education Commission of China, and the SICE Best Paper Award in 1994 from the Society of Instrument and Control Engineering of Japan at the 33rd SICE Annual Conference in Tokyo, Japan.

Thomas Kaiser (SM'04) received the diploma degree in electrical engineering from Ruhr-University Bochum, Bochum, Germany, in 1991 and the Ph.D. (with distinction) and Habilitation degrees in electrical engineering from Gerhard-Mercator-University, Duisburg, Germany, in 1995 and 2000, respectively.

From 1995 to 1996, he was on research leave with the University of Southern California, Los Angeles, supported by the German Academic Exchange Service. From April 2000 to March 2001, he was the Head of the Department of Communication Systems, Gerhard-Mercator-University. From April 2001 to March 2002, he was the Head of the Department of Wireless Chips and Systems, Fraunhofer Institute of Microelectronic Circuits and Systems, Duisburg. From April 2002 to July 2006, he was a Coleader of the Smart Antenna Research Team, University of Duisburg-Essen, Duisburg. In Summer 2005, he joined the Smart Antenna Research Group, Stanford University, Stanford, CA. In Winter 2007, he joined the Department of Electrical Engineering, Princeton University, Princeton NJ, as a Visiting Professor. Currently, he chairs the Communication Systems Group, Institute of Communication Technology, Faculty of Electrical Engineering and Computer Science, Leibniz University Hannover, Hannover, Germany. He is the Founder and the Chief Executive Officer of mimoOn GmbH. He is the author of more than 100 papers in international journals and conference proceedings. He has been a Guest Editor of several special issues and is a coeditor of four books on multiantenna and ultrawideband systems. He serves on the editorial board of the *EURASIP Journal of Applied Signal Processing*. He is involved in several national and international projects, has chaired and cochaired a number of special sessions on multiantenna implementation issues, and is a Technical Program Committee member of several conferences. His current research interest focuses on applied signal processing with emphasis on multiantenna systems, particularly its applicability to ultrawideband systems and on implementation issues.

Dr. Kaiser is a Member-at-Large of the Board of Governors of the IEEE Signal Processing Society. He was the Founding Editor-in-Chief of the e-letter of the IEEE Signal Processing Society. He was the General Chair of the IEEE International Conference on Ultra Wideband in 2008 and the General Chair of the International Conference on Cognitive Radio Oriented Wireless Networks and Communications in 2009.